

# Review and Prospect of PET/MR Dual Functional Tracer Development

高潘福、趙泓宇、吳世彥、趙啟民、劉冠妙

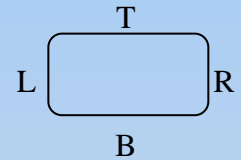
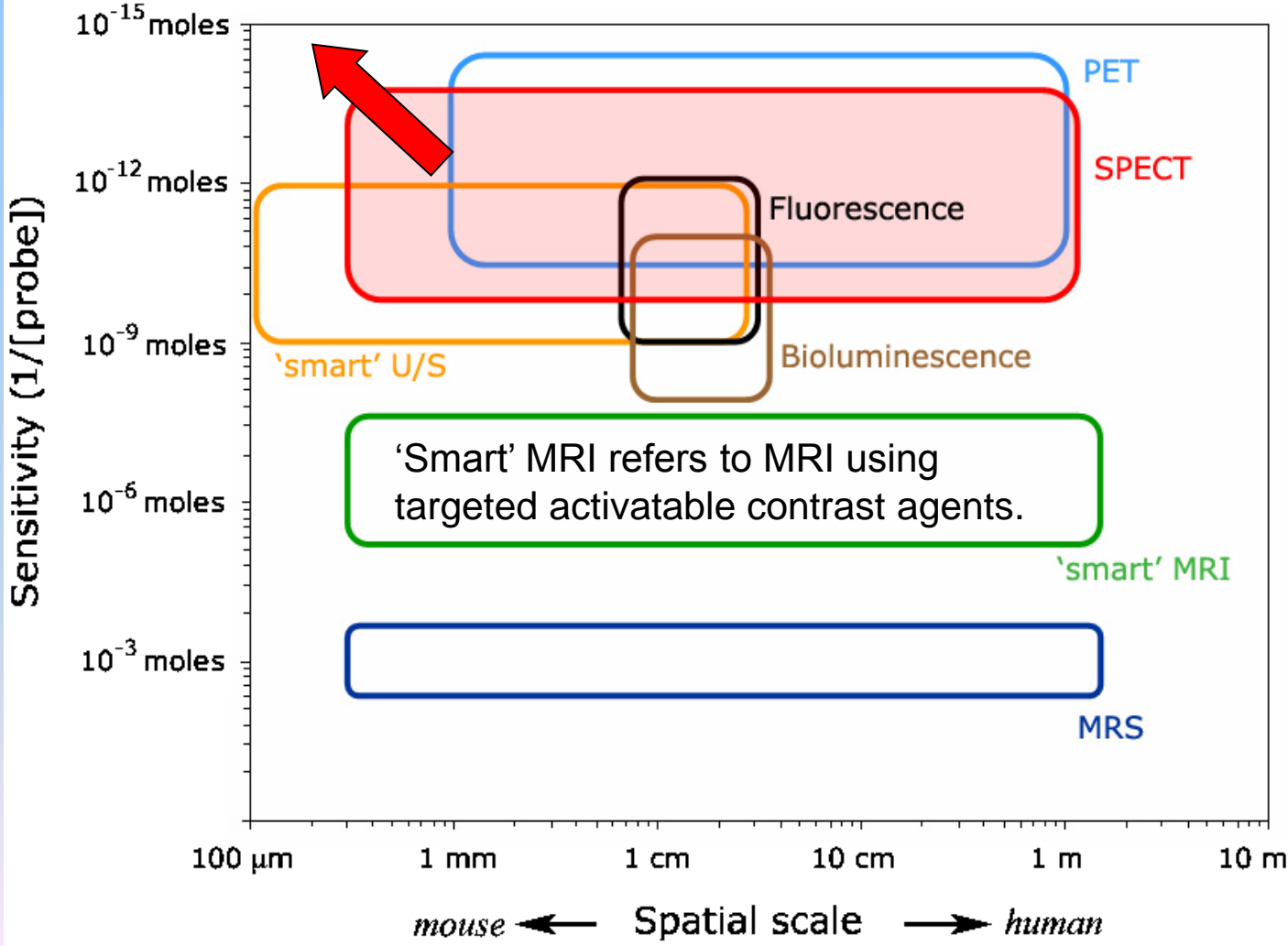
中山醫學大學 暨 附屬醫院

廖美秀

行政院原子能委員會 核能研究所

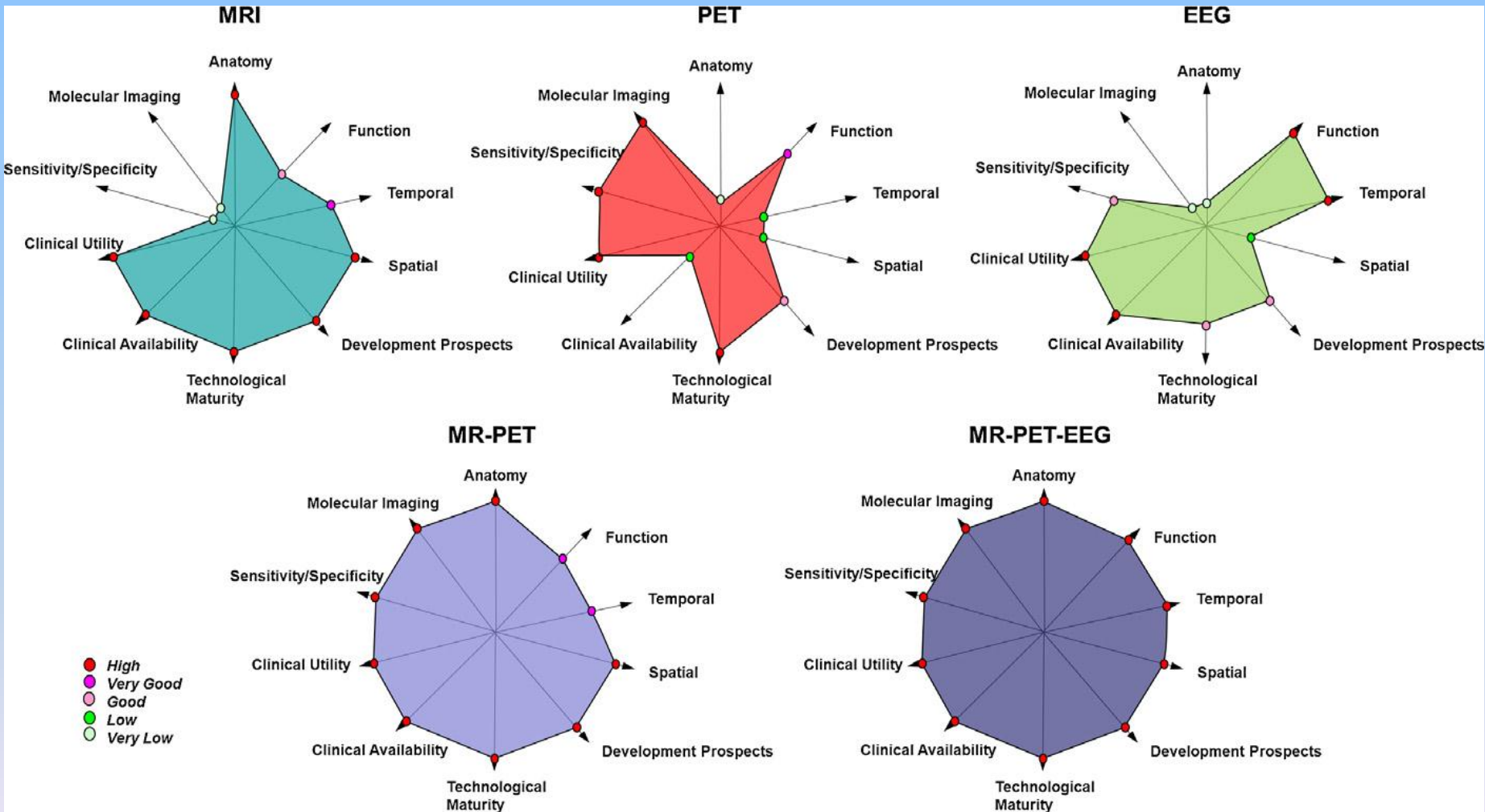
MOST 104- 2623-E-040-001-NU

# The Molecular Imaging Matrix of Pre-clinical Imaging Modalities

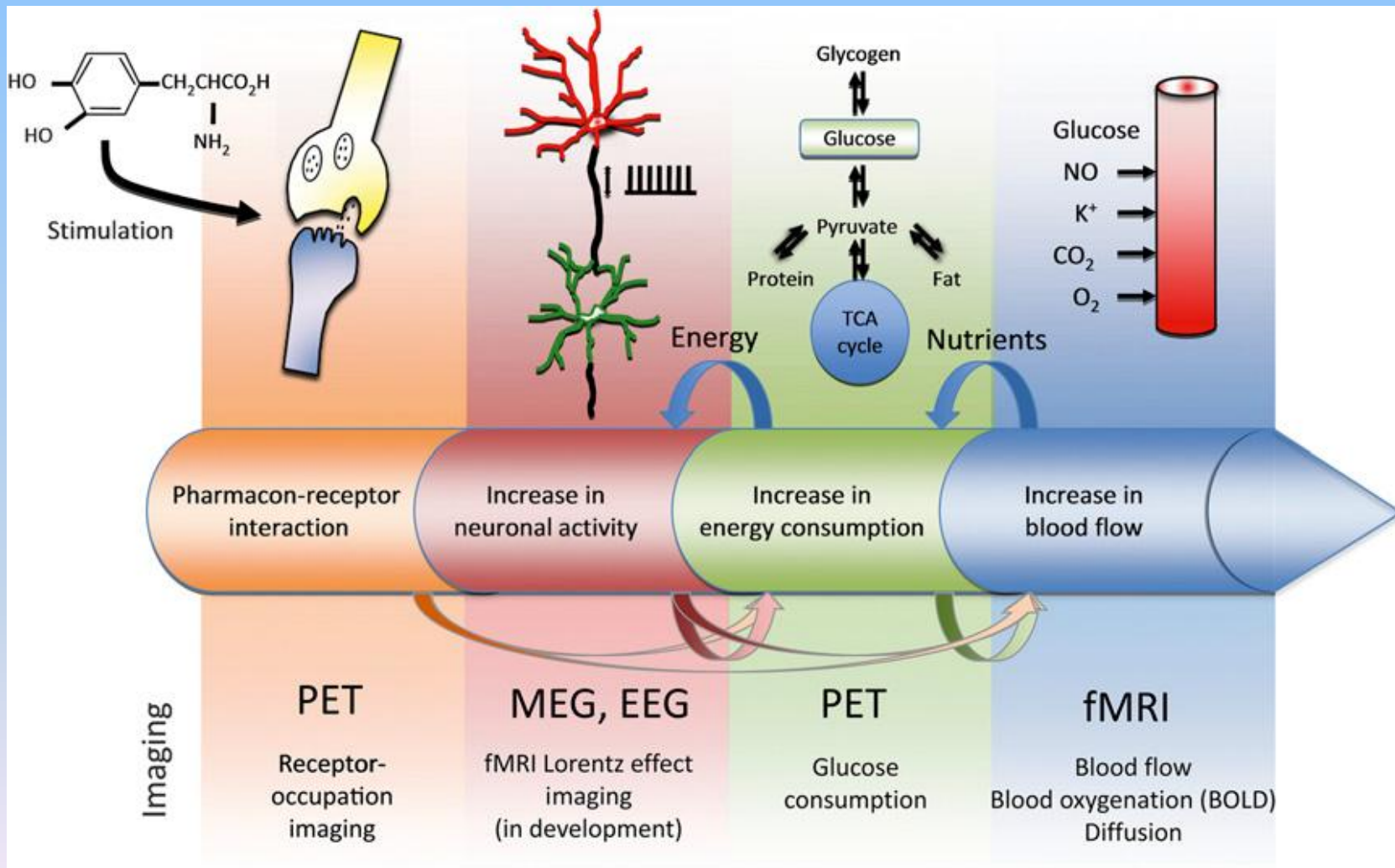


L: Limit of Resolution  
 R: Depth of Penetration  
 T: Sensitivity  
 T-B: Dynamic Range

Meikle et al., Phys. Med. Biol. 50 (2005) R45-R61.



J Magnetic Resonance 229 (2013) 101–115.



*J Nucl Med.* 2014;55:40S-46S.

# ***PET/MRI: Goes the Potential beyond Dual-Modality Imaging?***

The original aim of combining PET and MRI as a dual modality imaging system was to cover weaknesses of the existing PET/CT systems, which are lack of soft-tissue contrast and the relatively high radiation dose applied from the CT.

**However, MR imaging goes far beyond acquiring anatomical images with high-quality and high soft-tissue contrast; MRI offers also functional information such as fMRI and proton spectroscopy.** Thus, complementary functional information from PET and MRI can be correlated, providing additional information for kinetic modeling. The potential of simultaneous PET/MRI, therefore, goes beyond revealing tracer uptake and morphology towards multifunctional imaging.

Pichler BJ., et al. Multimodal Imaging Approaches: PET/CT and PET/MRI. In W. Semmler and M. Schwaiger (eds.), *Molecular Imaging I*. 109 Handbook of Experimental Pharmacology 185/I. Springer-Verlag Berlin Heidelberg 2008

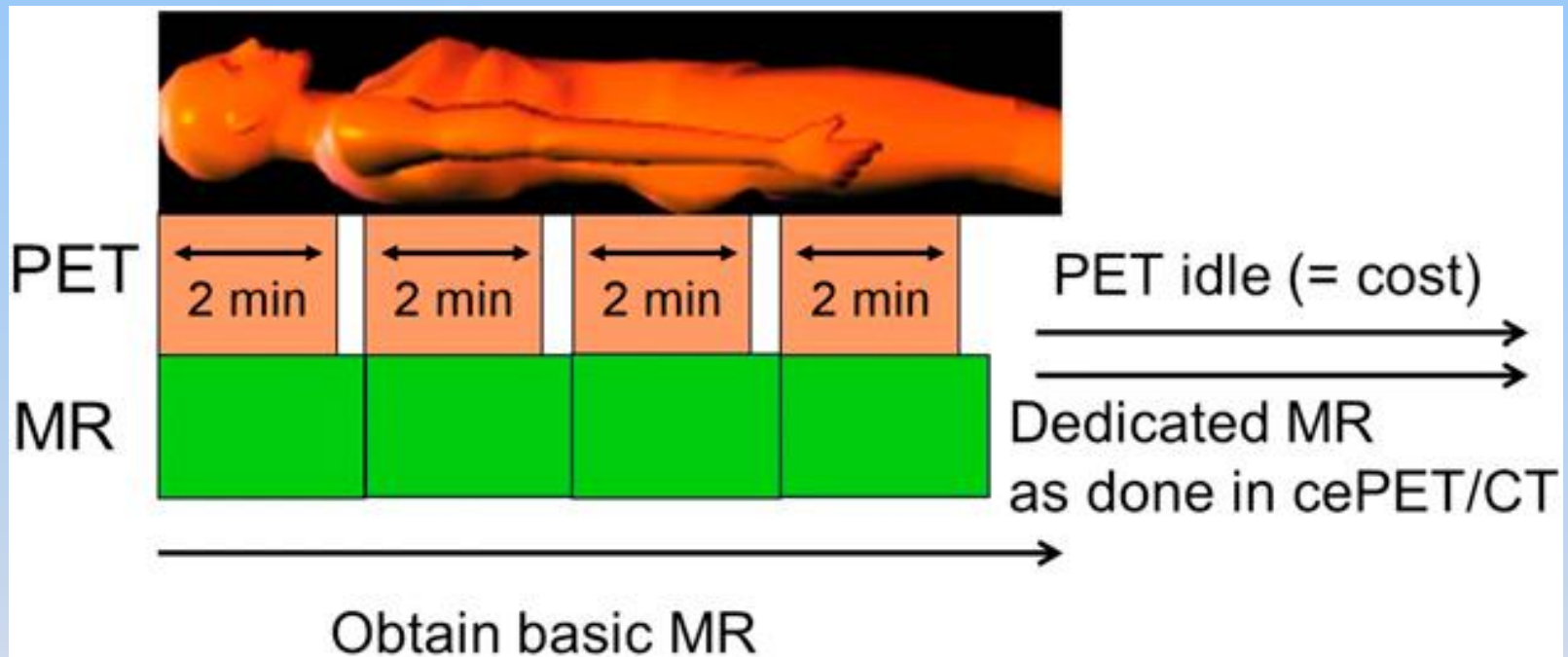
## Assessment of biological properties by MR and PET.

MR	PET
Morphology	Flow ( $H_2^{15}O$ )
Water diffusion capacity (DWI)	Metabolism ( $^{18}F$ -FDG)
Vascular anatomy (MRA)	Blood volume ( $C^{15}O$ )
Perfusion (PWI, DCE-MRI)	Oxygen consumption ( $^{15}O$ )
Tissue metabolites ( $^{13}C$ -labeled compound MRS)	Hypoxia ( $^{18}F$ -MISO)
Functional activation (fMRI)	Vascular permeability (labeled AA)
Cerebral fiber tracts (DTI)	Nuclide acid synthesis ( $^{18}F$ -FLT)
Oxygen consumption ( $^{17}O$ )	Transmitters (e.g. $^{18}F$ -DOPA)
Migration of cells (Fe labeling)	Enzymatic activity (e.g., MP4A) Enzymatic activity in transfected cells
	Angiogenesis (e.g. $^{18}F$ -RGD)
	Distribution and kinetics of tracers and drugs (labeled compounds)

**Table 1: Summary of commonly available functional MRI techniques, the quantitative parameters derived and their biological correlates.**

Functional Imaging Technique	Biological property on which imaging is based	Commonly derived quantitative imaging parameters/ biomarkers	Pathophysiological correlates
Diffusion-weighted MRI (DW-MRI)	Diffusivity of water	<ul style="list-style-type: none"> <li>■ Apparent diffusion coefficient (ADC)</li> <li>■ Fractional anisotropy (FA)</li> <li>■ Water diffusivity (D)</li> <li>■ Perfusion fraction (<math>F_p</math>)</li> </ul>	Cell density and distribution of cell sizes, extracellular space tortuosity, gland formation, cell membrane integrity, necrosis, fluid viscosity
Dynamic contrast-enhanced MRI (DCE-MRI)	Contrast medium uptake rate in tissues, which is influenced by: <ul style="list-style-type: none"> <li>■ Perfusion &amp; transfer rates</li> <li>■ Extra-cellular volume</li> <li>■ Plasma volume fraction</li> </ul>	<ul style="list-style-type: none"> <li>■ Initial area under gadolinium curve (IAUGC)</li> <li>■ Transfer and rate constants (<math>K^{trans}</math>, <math>k_{ep}</math>)</li> <li>■ Leakage space fraction (<math>v_e</math>)</li> <li>■ Fractional plasma volume (<math>v_p</math>)</li> </ul>	Vessel density Vascular permeability Perfusion Tissue cell fraction Plasma volume
Dynamic susceptibility contrast MRI (DSC-MRI)	Blood volume and blood flow	<ul style="list-style-type: none"> <li>■ relative blood volume/flow (rBV/rBF)</li> <li>■ Mean transit times (MTT)</li> <li>■ Vessel size index</li> </ul>	Vessel density Blood flow Tumor grade Vessel diameter
$^1\text{H}$ -MR spectroscopic imaging ( $^1\text{H}$ -MR-SI)	Cell membrane turnover/energetics and replacement of normal tissues	<ul style="list-style-type: none"> <li>■ Quantified ratios of metabolites including choline, creatine, lipids, citrate, lactate and others depending on echo time and tissues evaluated</li> </ul>	Tumor grade Proliferation index
Blood oxygenation level dependent (BOLD) or intrinsic susceptibility-weighted (ISW) MRI	Deoxyhaemoglobin shows higher relaxivity than oxyhaemoglobin. Measurement also reflect blood volume, perfusion and Intrinsic composition of tissues	<ul style="list-style-type: none"> <li>■ Intrinsic tissue relaxation rate (<math>R2^* = 1/T2^*</math>)</li> </ul>	Tissue susceptibility properties including air and bone interfaces, ferromagnetic properties and blood oxygenation



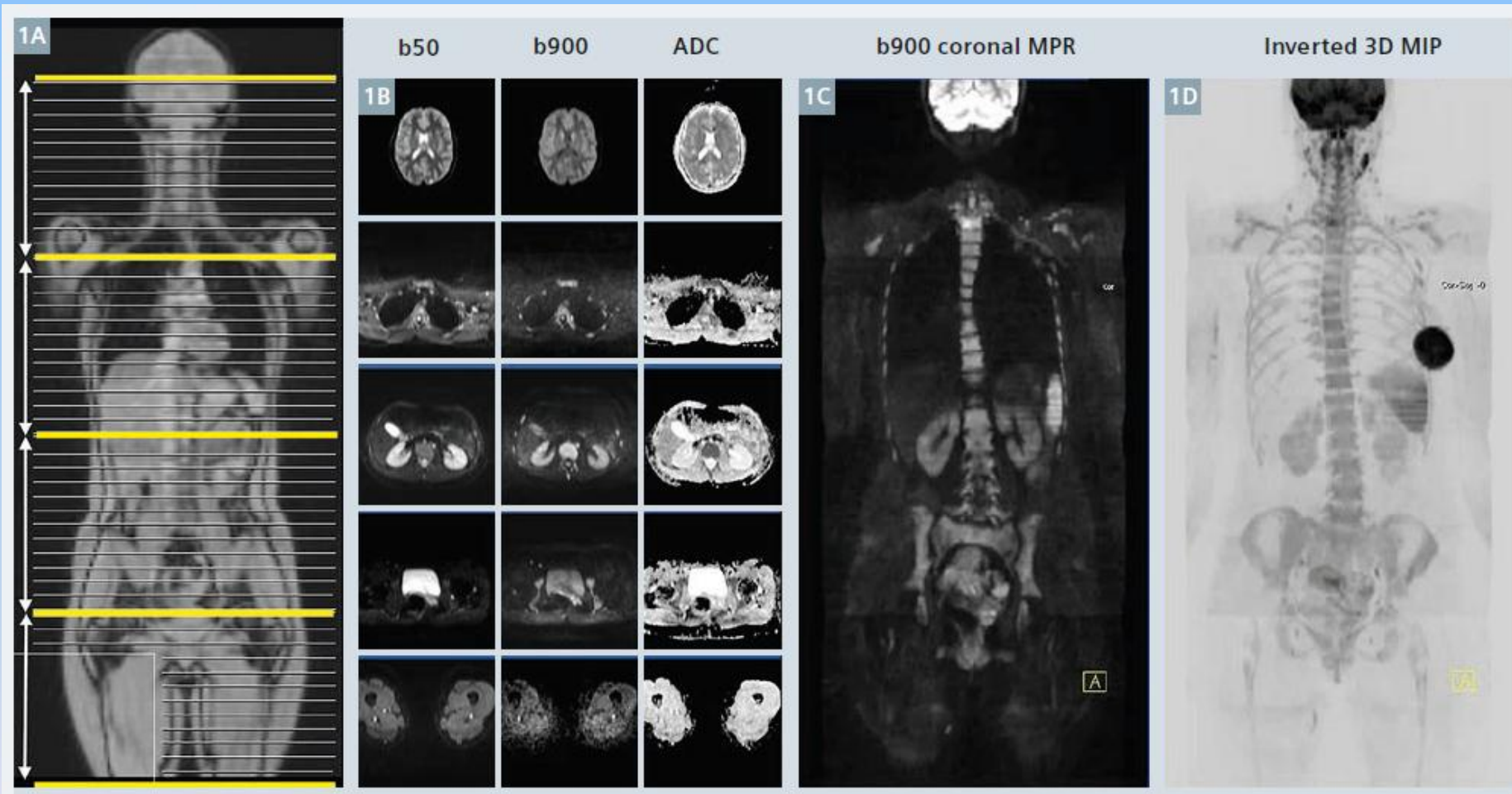


Schematic of PET/MR whole-body data acquisition.  
 Transaxial field of view: 15–25 cm.

J Nucl Med 2014; 55:19S–24S.



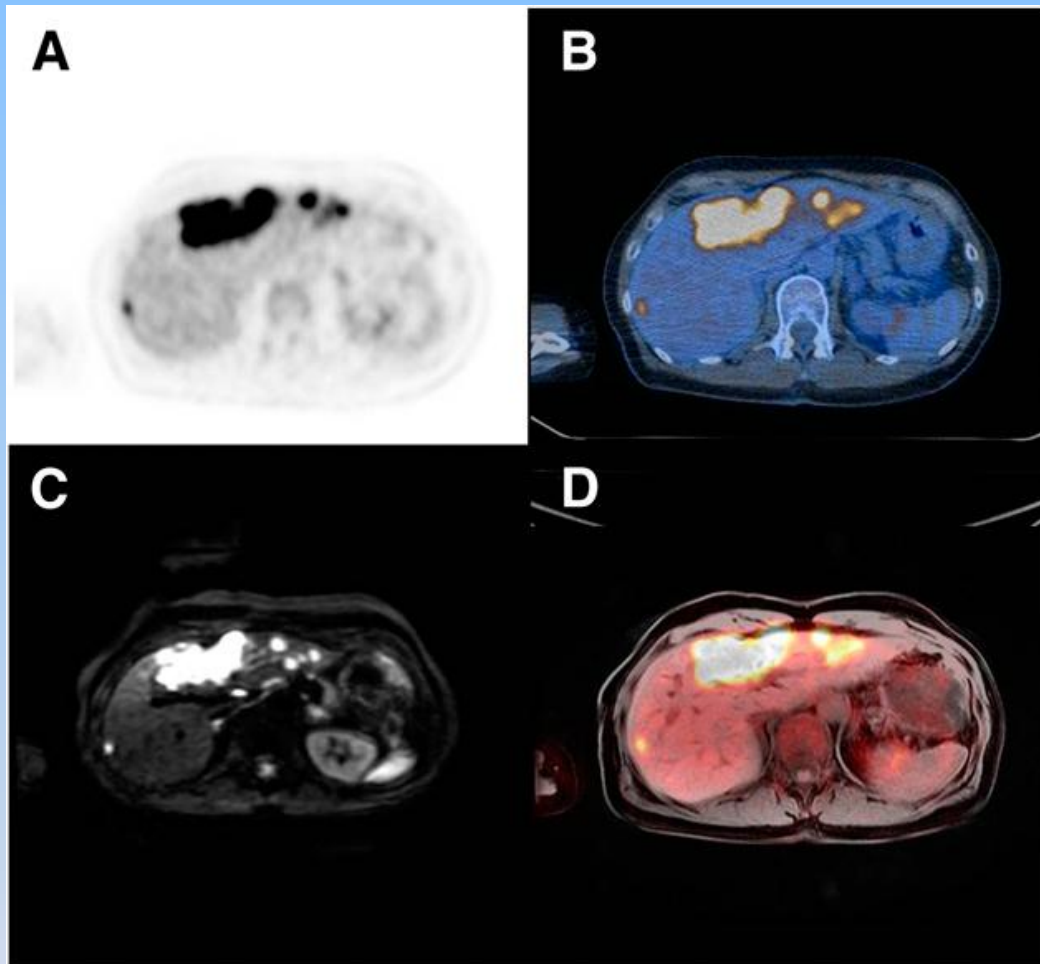
# Whole Body Diffusion-Weighted MRI for Bone Marrow Tumor Detection



**WB-DWI workflow.** 27-year-old woman with sarcomatoid left breast cancer. The bone marrow pattern is normal for age. Axial DWI from the skull base to the mid-thigh is performed using 2 b-values (50 and 900 s/mm<sup>2</sup>) with a slice thickness of 5 mm in 4 stations. The b900 images are reconstructed into the coronal plane (5 mm) and displayed as thick 3D MIPs (inverted grey scale). ADC images are computed inline with mono-exponential fitting of b50 and b900 signal intensities. MAGNETOM Flash | 4/2013 | [www.siemens.com/magnetom-world](http://www.siemens.com/magnetom-world)

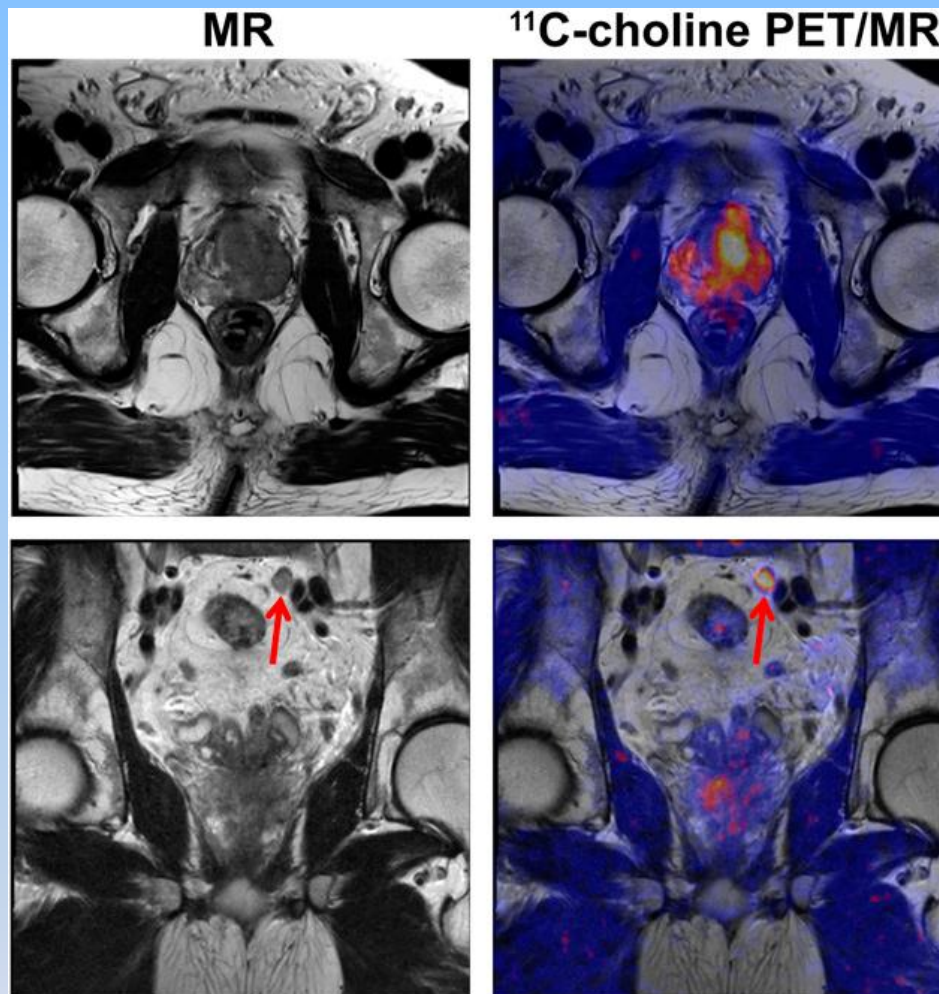


**5 Improved lymphoma staging with whole-body  $^{18}\text{F}$ FDG-PET and DW-MRI.** 23-year-old male with Hodgkin's lymphoma. Nodal distribution of disease between whole-body  $^{18}\text{F}$ FDG-PET and DW-MRI is very similar. The  $^{18}\text{F}$ FDG-PET scan shows a splenic deposit (arrow on the PET scan) which is not visible on the DW-MRI (where only normal increased signal intensity is seen). On the other hand the bone marrow abnormality seen in the left superior pubic ramus on the DW-MRI (arrow) is not appreciated on the PET scan. Both lesions were unproven histologically because their presence does not affect the therapy to be given. There is some variation in the signal intensity of the top station of the DW-MRI compared to the middle and lower stations.



Patient with disseminated liver metastases in both liver lobes: FDG PET only (A); PET/CT (B); diffusion-weighted MR imaging (C); PET/MR imaging (D). Liver metastases are clearly seen on PET/CT as well as on PET/MR imaging. MR imaging also shows lesions in both liver lobes but does not contribute to diagnostic accuracy.

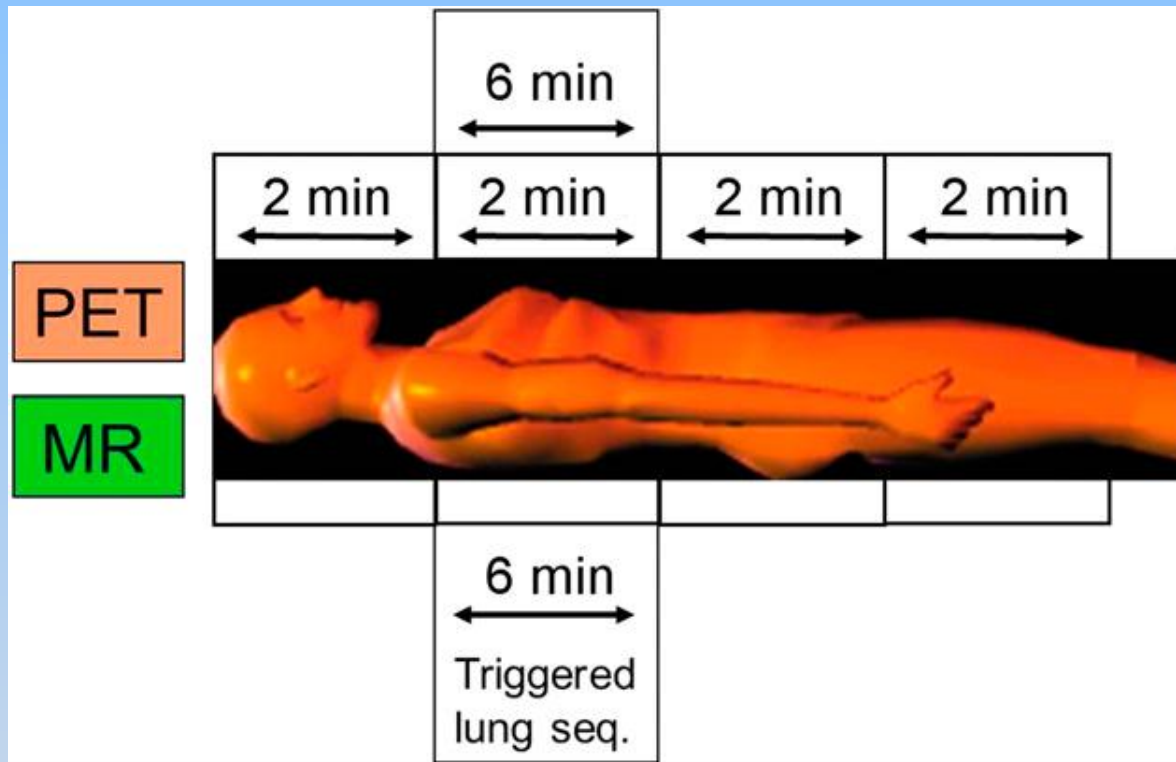
J Nucl Med 2014; 55:19S–24S.



A 58-y-old man with prostate cancer. <sup>11</sup>C-choline PET/MR image shows primary cancer in prostate gland (upper row) as well as pelvic lymph node metastasis (bottom row, arrow). This example emphasizes value of PET/MR imaging in oncologic diagnostics because high-resolution MR imaging can be combined with specific PET tracers.

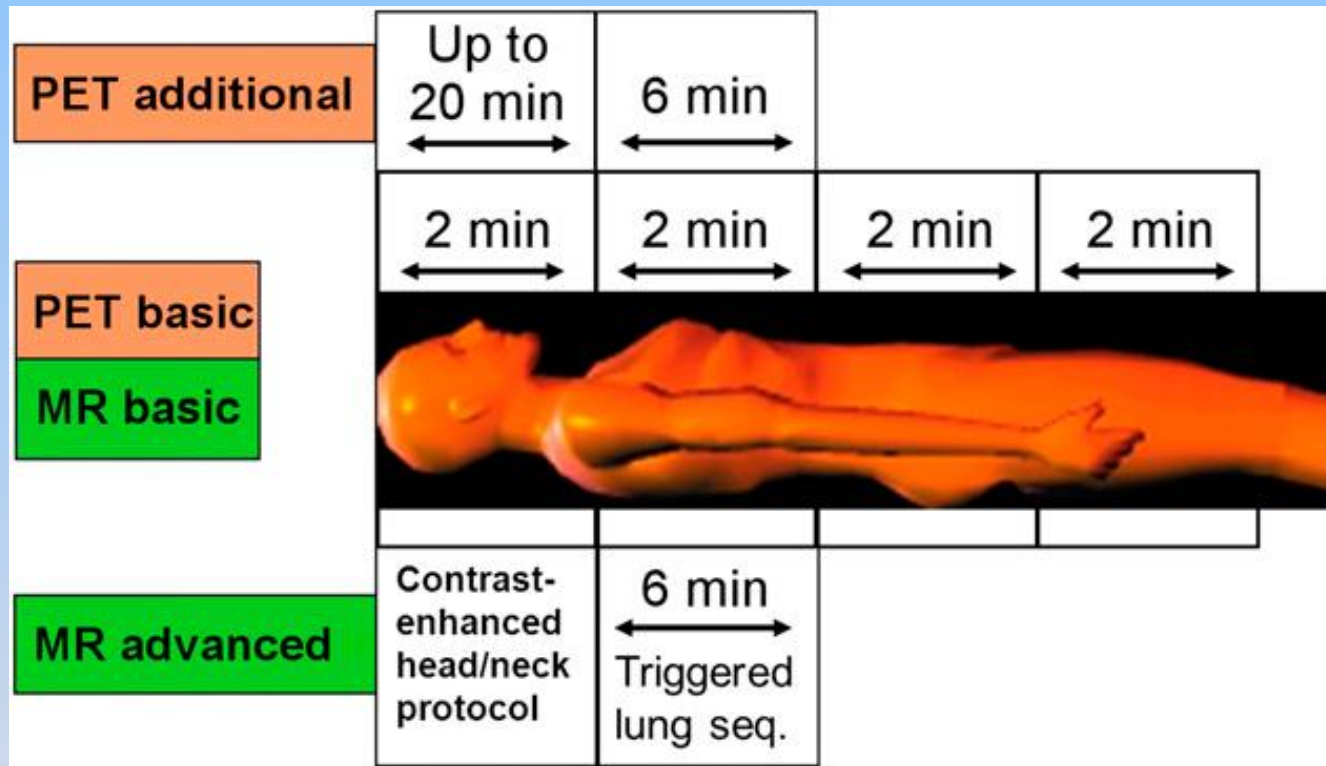
*J Nucl Med.* 2014;55:40S-46S.





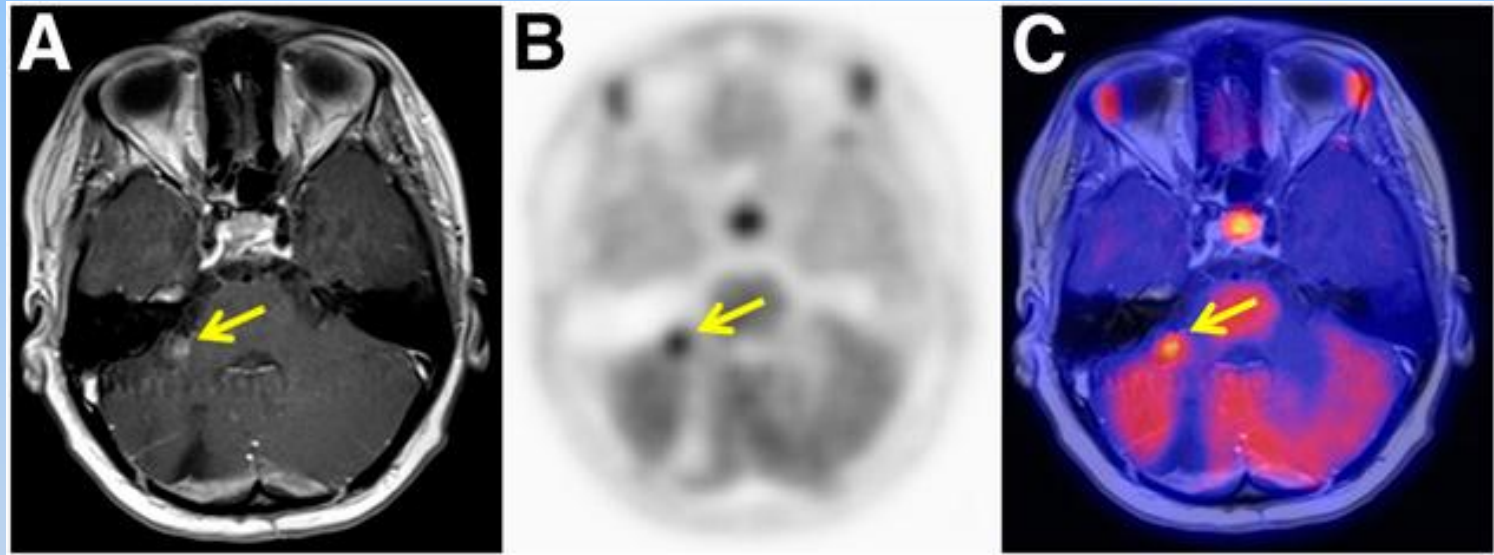
Schematic of possible basic PET/MR imaging partial-body data acquisition with triggered lung imaging. In MR imaging, Dixon T1-weighted and coronal T2-weighted fast spin-echo images would be acquired in 2 min per bed position. Additionally, **triggered lung sequence can be acquired, ideally with triggered PET acquisition (additional 4–6 min)**. Such a protocol would still be acquired in 15–17 min and thus be comparable to standard PET/CT acquisition.

# Advanced Whole-Body Protocols



Schematic of possible advanced PET/MR imaging partial body data acquisition with triggered lung imaging and additional contrast-enhanced MR imaging in one or two body compartments. This additional MR imaging acquisition typically adds up to 20–25 min of imaging time. One must decide whether this should be simultaneous with PET or MR imaging alone.

J Nucl Med 2014; 55:19S–24S.



Fourteen-year-old girl with history of post resection and radiotherapy of glioblastoma multiforme of right cerebellum. (A) T1-weighted MR imaging of brain shows contrast-enhanced suspect lesion (9 · 9 mm) in right cerebellar peduncle (arrow). (B and C) Simultaneous <sup>11</sup>C-methionine PET/MR imaging shows focal enhanced amino acid metabolism in this lesion, highly suggestive of tumor tissue. Histology confirmed glioblastoma relapse.

J Nucl Med 2014; 55:32S–39S.



# MRI Contrast Agents

- Approximately 35% of all clinical MRI scans utilize contrast agent.
- Require high concentrations that vary from 0.1 to 0.6 mM.
- Metals with magnetic moments ( $\text{Gd}^{+3}$ ,  $\text{Mn}^{+2}$ , and  $\text{Fe}^{+3}$ ) are effective contrast agents.

## Danger of 'gadolinium phobia' looms in Europe

By Philip Ward, AuntMinnie.com staff writer

March 4, 2016

VIENNA - There's a serious risk of a phobia developing over the use of gadolinium-based MRI contrast agents, following the recent publication of a stinging attack on these agents in a German newspaper, ECR 2016 delegates were told at Friday's highly charged special focus session on brain hypersignals after repeated gadolinium administrations.

The article, headlined "Beim MRT lagert sich Metall im Gehirn ab" (When MRI metal is deposited in the brain), was published on 8 February 2016 in the *Die Welt* newspaper. It reported that doctors have warned that MRI examinations using contrast should be abandoned, especially in children and adolescents, unless they are absolutely necessary.



*Avoid gadolinium phobia, urges Dr. Alexander Radbruch.*

At Friday's session, Dr. Alexander Radbruch, a radiologist at Heidelberg University Hospital in Germany, expressed strong concern about the article's attempt to link gadolinium deposition with Alzheimer's disease or dementia and the suggestion that cardiovascular MRI should be replaced by myocardial scintigraphy.

"Have a guess who made this recommendation -- it was obviously a nuclear medicine guy!" said Radbruch, who received the Coolidge Award in 2013 from GE Healthcare for his work on the use of new imaging techniques in brain cancer diagnostics. "There is absolutely no evidence at all of this. Radiologists really should try to avoid gadolinium phobia that would lead to an unreasonable decline of gadolinium-based contrast agents [GBCAs]."

Received 04 September 2013,

Accepted 29 October 2013

Published online 7 January 2014 in Wiley Online Library

(wileyonlinelibrary.com) DOI: 10.1002/jlcr.3154

# Potential clinical applications of bimodal PET-MRI or SPECT-MRI agents<sup>†</sup>

Rafael T. M. de Rosales\*

The introduction to the clinic of positron emission tomography-magnetic resonance imaging scanners opens up the possibility to evaluate the real potential of bimodal imaging agents. In this mini-review, the limitations in the design and applications of these materials are summarised and the unique properties that may result in real clinical applications outlined.

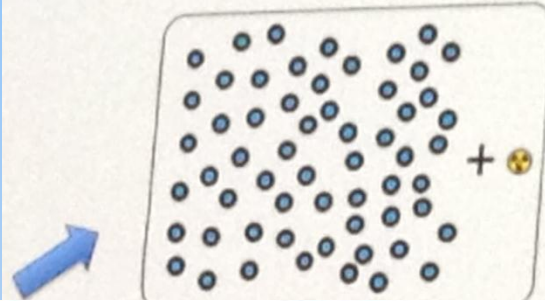
**Keywords:** medical imaging; PET-MRI; SPECT-MRI; multimodal agents; SPIO

Rafael T. M. de Rosales\*

Department of Imaging Chemistry & Biology, Division of Imaging Sciences and Biomedical Engineering, King's College London, UK

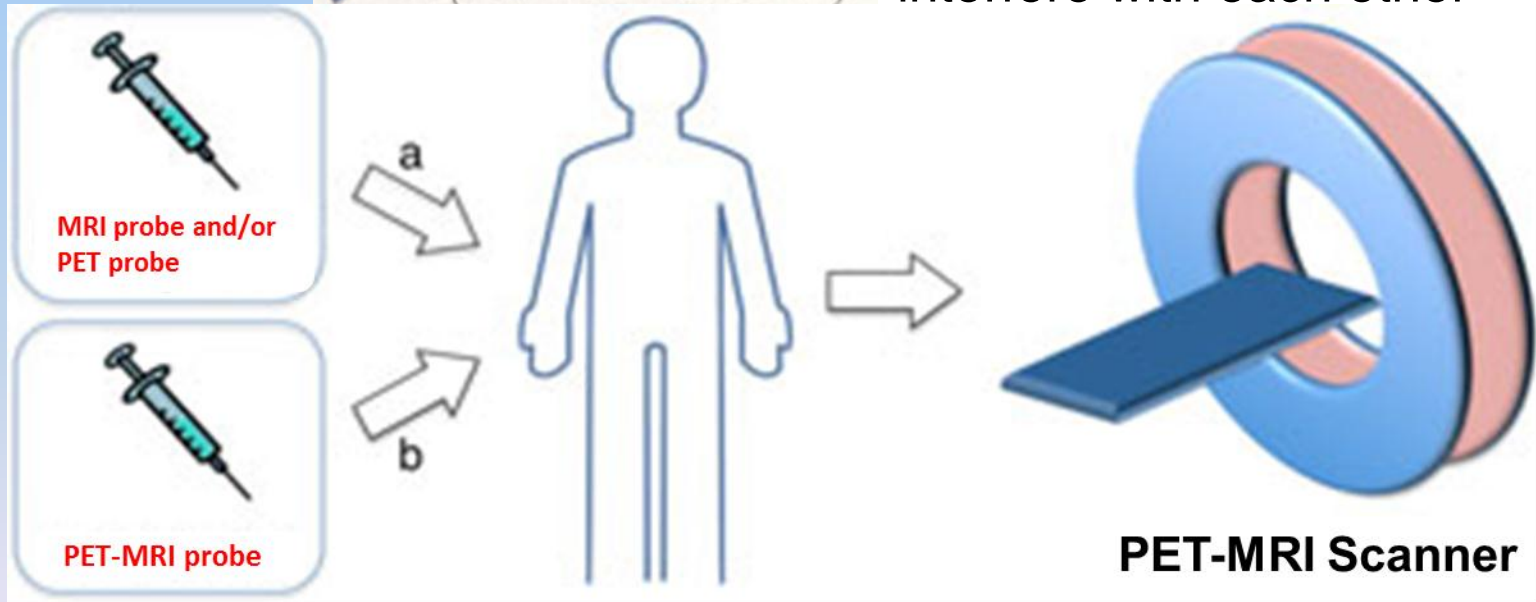
J. Label Compd. Radiopharm 2014, 57 298–303.

# Imaging Agents for PET/MR



Multiparametric  
Complementary  
Information

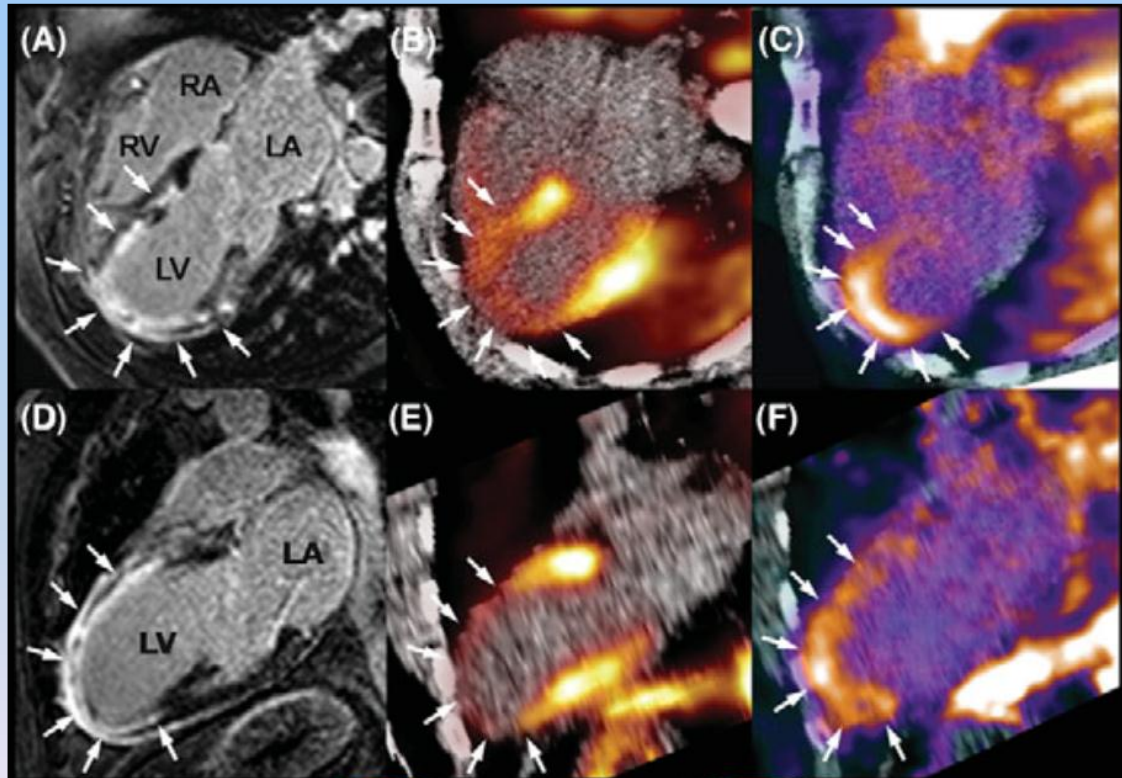
Contrast agents should not  
interfere with each other



J. Label Compd. Radiopharm 2014; 57 :298–303.

# Contrast Agent and PET/MR myocardial infarction

MRI Gd-DTPA      PET [N-13]Ammonia      PET [F-18]Galakto-RGD)



Delayed Gd  
enhancement  
scar tissue

Perfusion

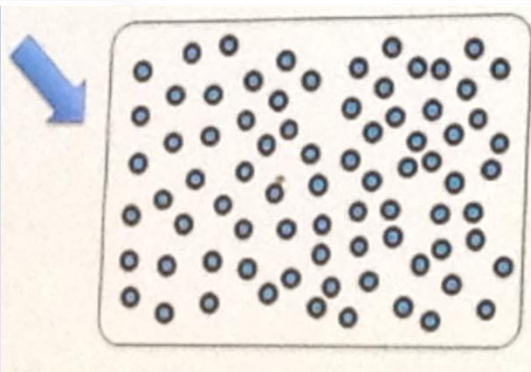
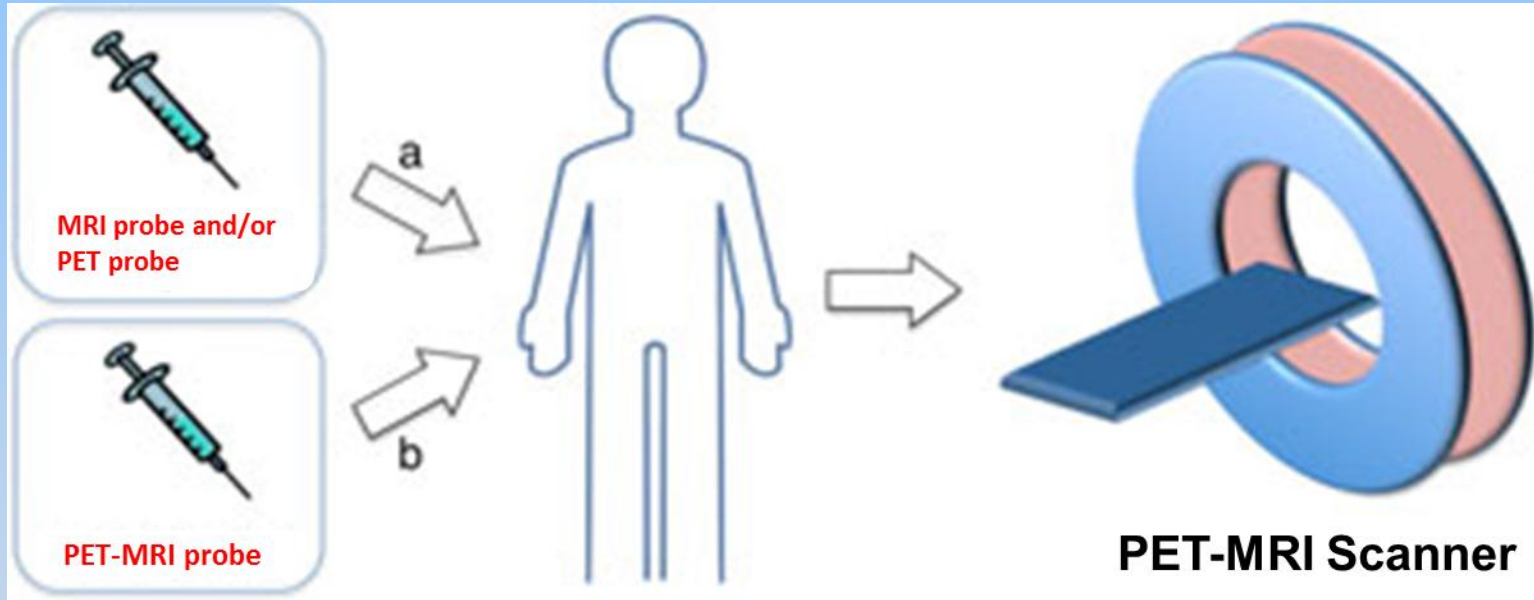
Angiogenesis?  
tissue regeneration

Eur Heart J 2008;29:2201.

A 35-year-old  
Caucasian male  
presented with  
chest pain and  
nausea in the  
emergency room....



# Imaging Agents for PET/MR



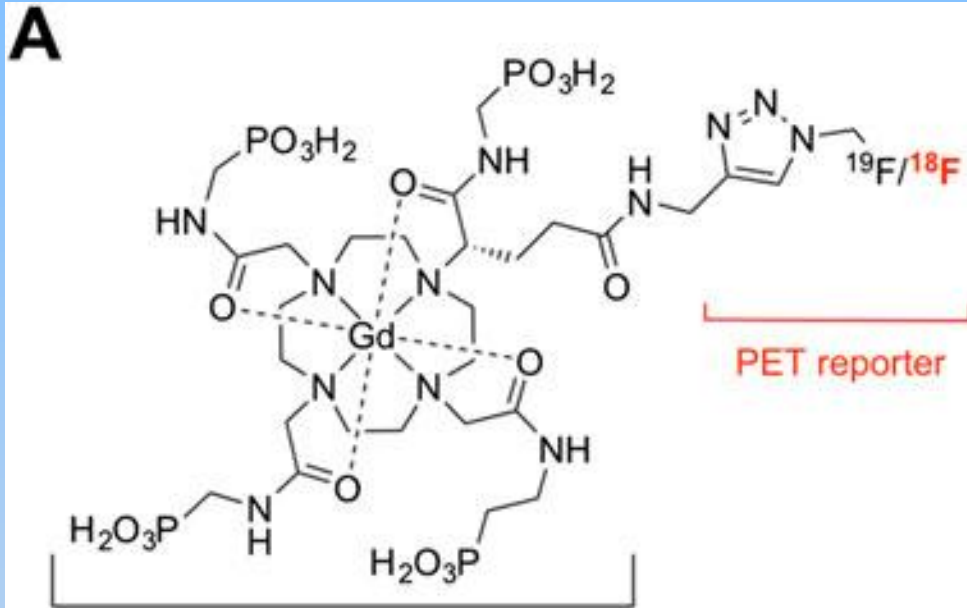
- Very low specific activity
- Not useful for molecular imaging unless highly-abundant targets
- Radiolabeled and non-radiolabeled must show same behavior

J. Label Compd. Radiopharm 2014; 57 :298–303.

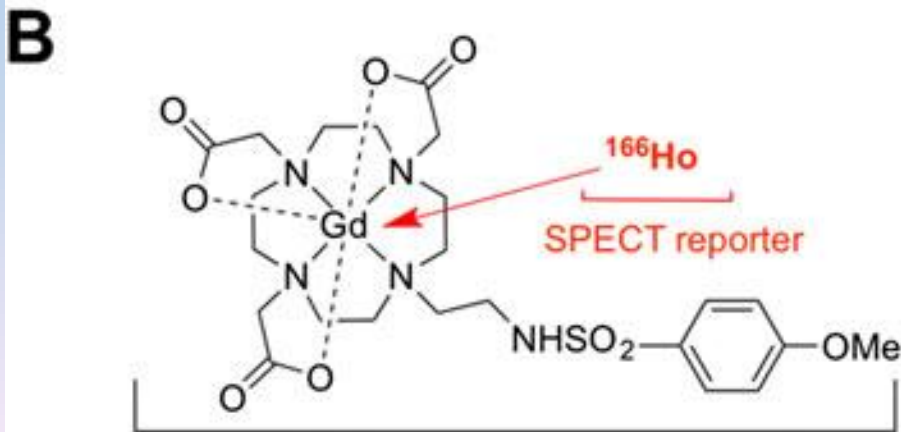
# MRI Contrast Agents

- Paramagnetic agent ( $\text{Gd}^{+3}$ -DTPA): enhance T1-weighted images by shortening the T1-relaxation time in water.
- Super paramagnetic agent (iron oxide core, Fe/Mn composition metal core, covered in a polymer matrix to prevent aggregation and to form a larger magnetic moment): shortening the T2-relaxation time.
- To localize tumor and quantifying their size.





pH-sensitive MRI reporter



pH-sensitive MRI reporter

One of the great properties of MRI contrast agents is that they can be designed to be responsive (i.e. changes in relaxivity or 'signal intensity') to external factors such as pH. The clinical relevance of such probes is that pH is a potential biomarker of tumours and other tissues. In both cases, the positron emission tomography/single photon emission computed component is used to **calculate the concentration of the contrast agent, making the pH measurement** using the magnetic resonance imaging component possible.

J. Label Compd. Radiopharm 2014; 57 :298–303.

# 放射磁性金屬PET/MR顯影劑

- Fe, Gd, Mn有MRI磁性顯影功能
- 其可行 $\beta^+$ 放射的同位素推測有PET/MRI顯影的功能

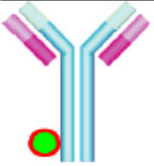


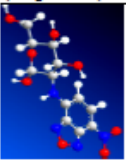
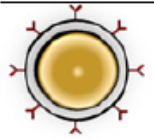
Atom	Z	T1/2	decay mode	PubMed
Mn	51	46.2 m	$\beta^+ \rightarrow$ Cr-51	7
Mn	52m	21.1 min	$\beta^+$ (98.25%) $\rightarrow$ Cr-52	12
Gd	147	38.06 h	$\beta^+$	4

# 放射磁性金屬PET/MR顯影劑

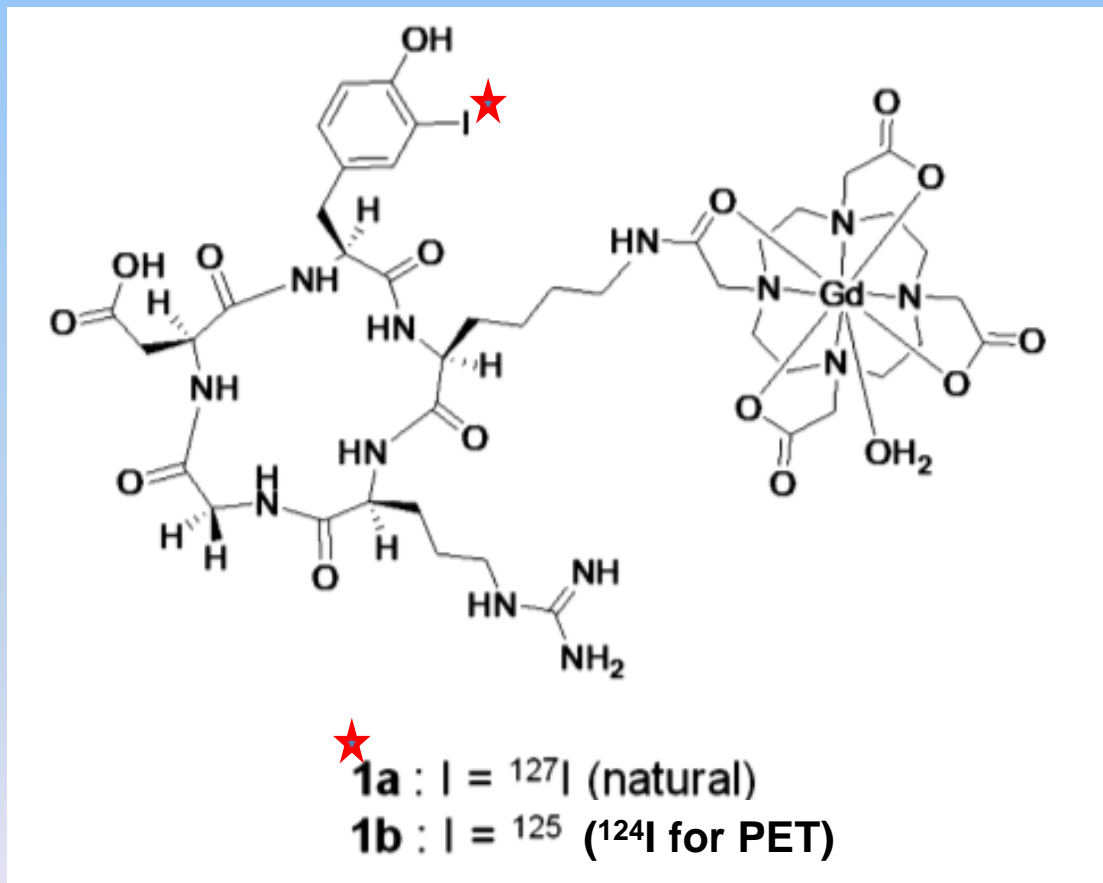
- Mn-51, Mn-52m的製備需要很大的能量
- Mn MRI顯影劑的生物性質不佳
- Gd-147需要強子對撞機(Hadron Collider)

Atom	Z	T1/2	decay mode	PubMed
Mn	51	46.2 m	$\beta + \rightarrow$ Cr-51	7
Mn	52m	21.1 min	$\beta +$ (98.25%) $\rightarrow$ Cr-52	12
Gd	147	38.06 h	$\beta +$	4

# Various ligands for imaging in different molecular imaging modalities.

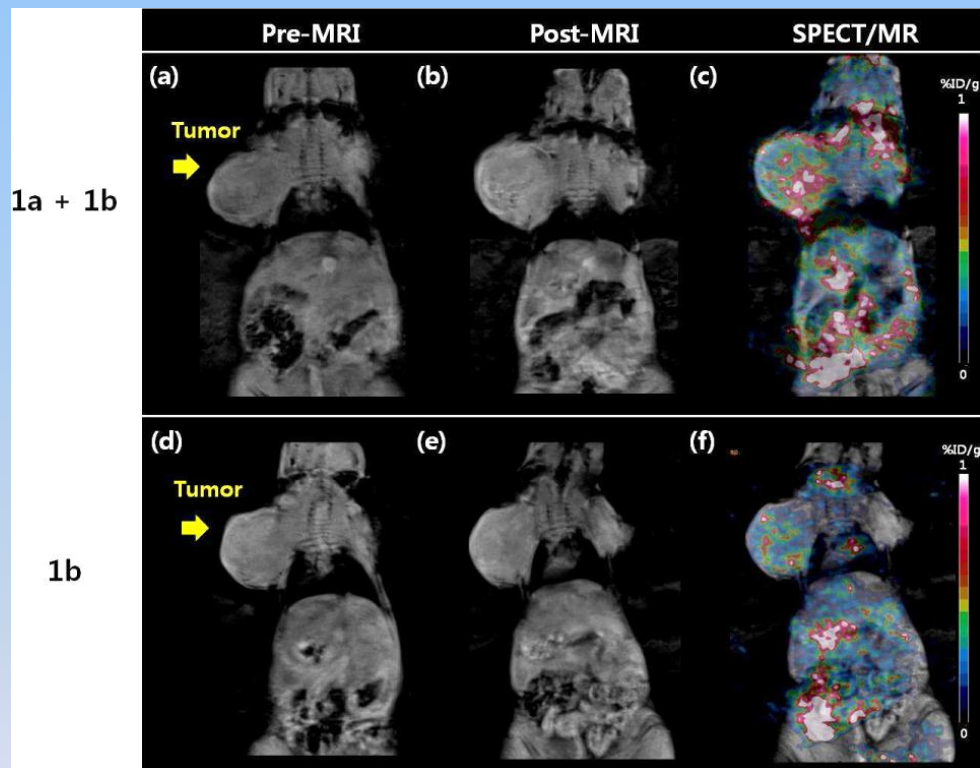
Detection ligand	Advantages	Disadvantages
 (Antibody)	<ul style="list-style-type: none"> <li>• Low antigenicity and acceptable toxicity and high specificity to targets.</li> <li>• Many clinically approved antibodies available for labeling.</li> </ul>	<ul style="list-style-type: none"> <li>• Long blood half-life decreases specificity of signal.</li> </ul>
 (Antibody fragments)	<ul style="list-style-type: none"> <li>• These structures retain high binding affinity and specificity. Clearance times well-suited for imaging.</li> </ul>	<ul style="list-style-type: none"> <li>• More complex to formulate compared to whole antibodies.</li> </ul>
 (Peptides)	<ul style="list-style-type: none"> <li>• High specificity to targets, easy for synthesis and feasible for conjugation with contrast agents, rapid clearance times.</li> </ul>	<ul style="list-style-type: none"> <li>• Many peptides have brief serum half-lives, usually caused by degradation or excretion.</li> </ul>
 (Small molecules)	<ul style="list-style-type: none"> <li>• High specificity, rapid clearance. Intra-cellular targets are available for imaging.</li> </ul>	<ul style="list-style-type: none"> <li>• Fluorochromes and their comparable size to small molecules may affect pharmacokinetics and biodistribution of the resulting labeled ligands.</li> </ul>
 (Nanoparticles)	<ul style="list-style-type: none"> <li>• Can be used for multi-valent targeting, strong fluorescence, broad and narrow excitation bands, tunable fluorescence, and ideal for efficient modification due to large surface area.</li> </ul>	<ul style="list-style-type: none"> <li>• Long term toxic effects generated by tracers of heavy metals, requires long clearance times.</li> </ul>

# Peptides and Small Molecules



Kim KM, et al. Gadolinium Complex of <sup>125</sup>I/<sup>127</sup>I-RGD-DOTA Conjugate as a Tumor- Targeting SPECT/MR Bimodal Imaging Probe. ACS Med. Chem. Lett. 2013, 4, 216

# Conjugate as a Tumor-Targeting SPECT/MR Bimodal Imaging Probe



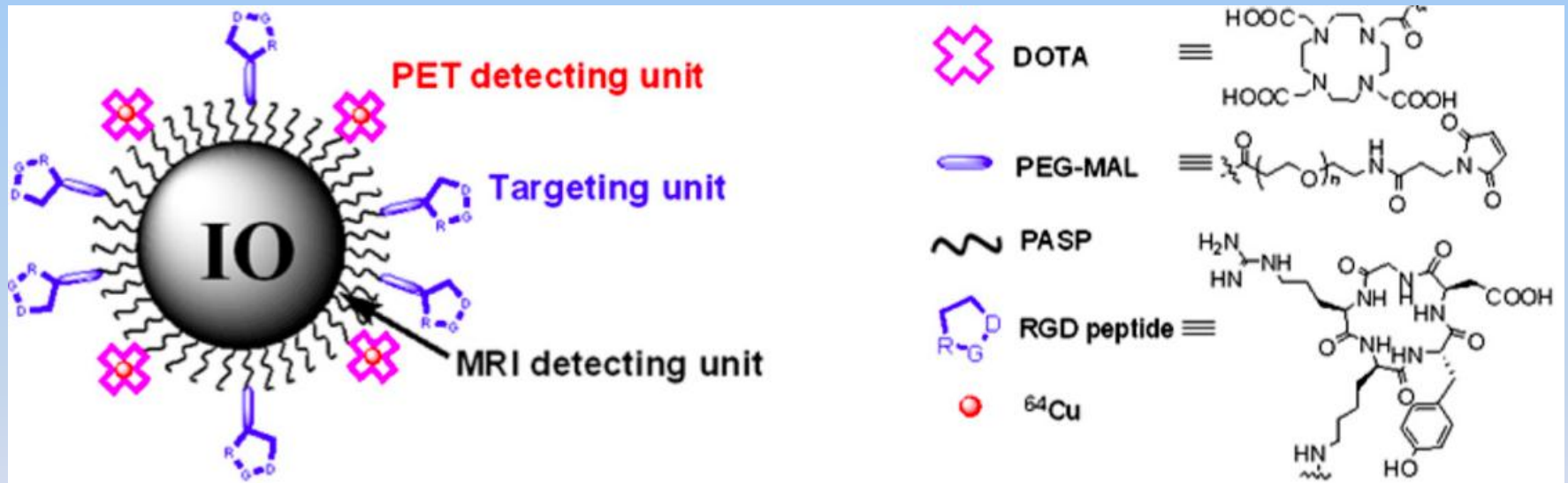
To overcome the sensitivity difference, the relative amounts of 1a and 1b were adjusted as follows: [1a] for MRI = 2.7 mg (0.1 mmol Gd/kg); [1b] for SPECT =  $1.5 \times 10^{-5}$  mg (200  $\mu$ Ci).

In vivo MR and SPECT/MR images of U87MG tumor bearing mice obtained with a mixture of 1a and 1b (a–c) and 1b (d–f). Quantitative analyses of SPECT imaging of tumors were  $0.56 \pm 0.05$  and  $0.24 \pm 0.09$  at c and f, respectively.

Kim KM, et al.. ACS Med. Chem. Lett. 2013, 4, 216.

# Iron Oxide Nanoparticle (IONPs)

superior magnetic properties, ease of modification, biocompatibility

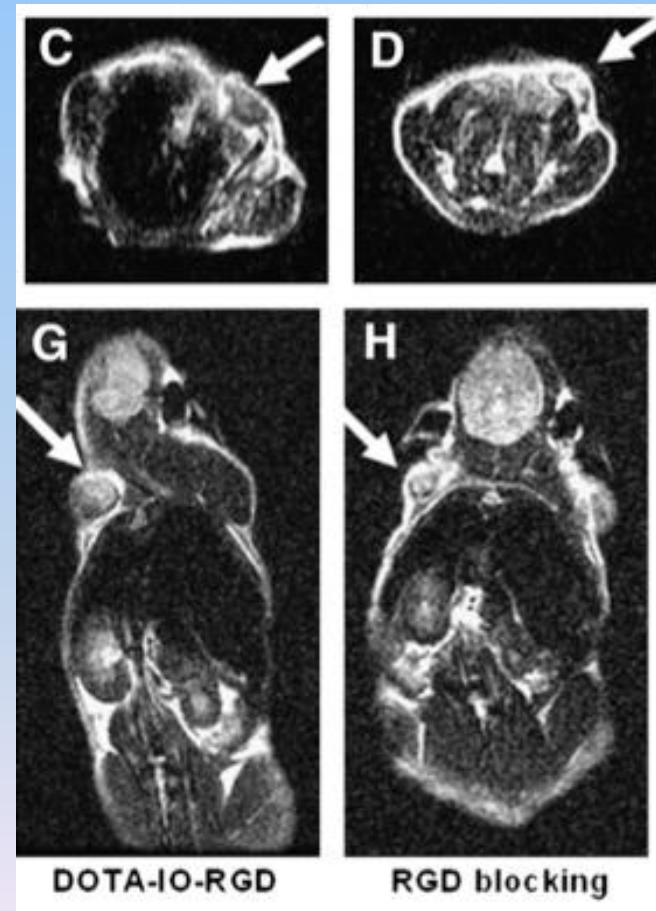
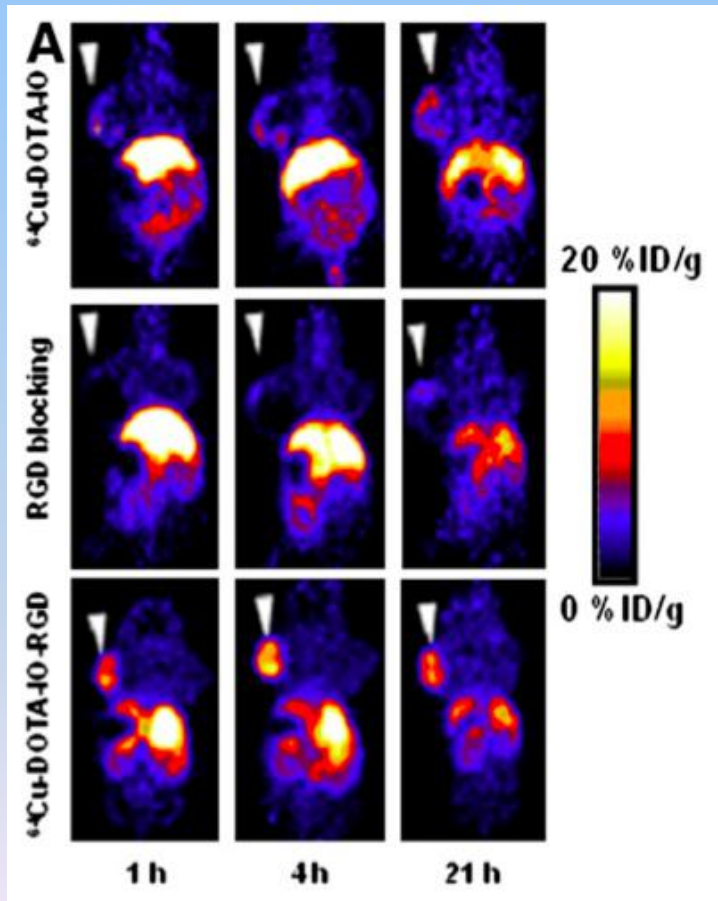


## (RGD)-Conjugated Radiolabeled Iron Oxide Nanoparticle

Chen X, et al. *PET/MRI Tumor Imaging Using Arginine-Glycine-Aspartic (RGD)-Conjugated Radiolabeled Iron Oxide Nanoparticles*, *J Nucl Med.* 2008;49:1371

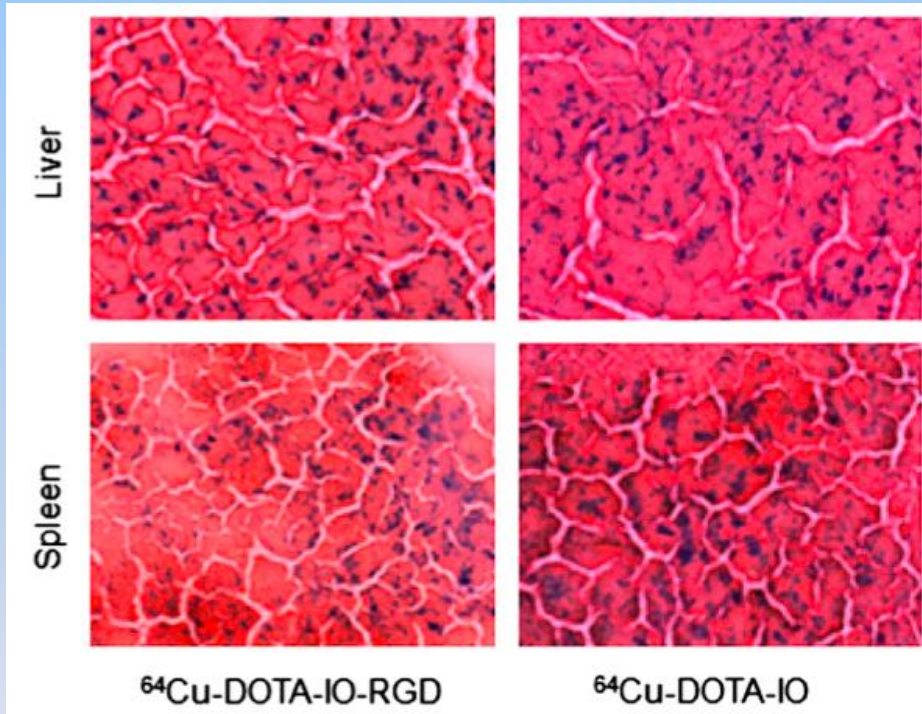


- rat PET and T2 MRI show specific delivery RGD-PASP-IO



Chen X, et al. *J Nucl Med.* 2008;49:1371

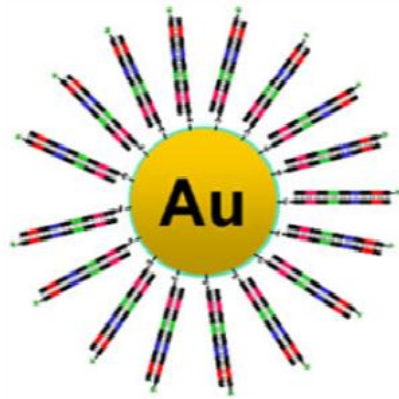
# *RGD–Conjugated Radiolabeled Iron Oxide Nanoparticle*



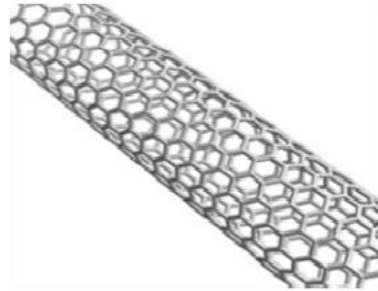
*J Nucl Med.* 2008;49:1371.

Accumulation in  
liver, spleen, and  
kidneys

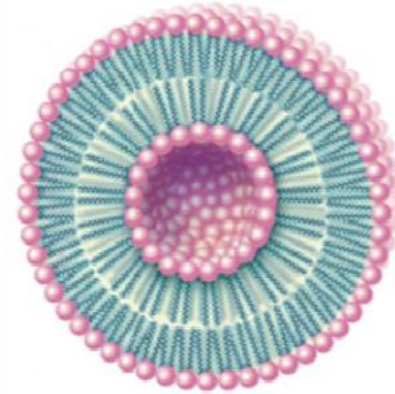
*Nanoparticles for cancer imaging: The good, the bad, and the promise, Sandra C. Nano Today.* 2013 ; 8(5): 454



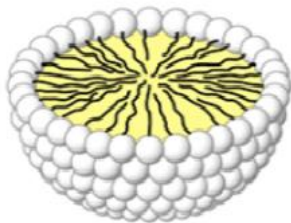
(A)



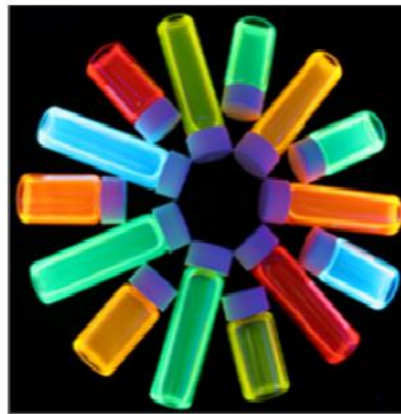
(B)



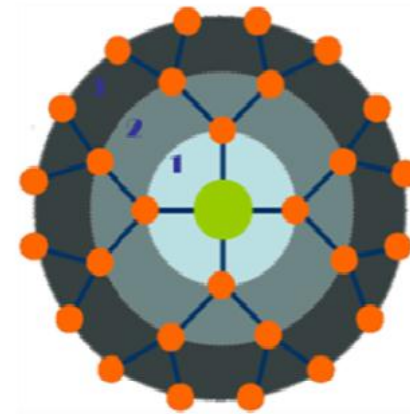
(C)



(D)



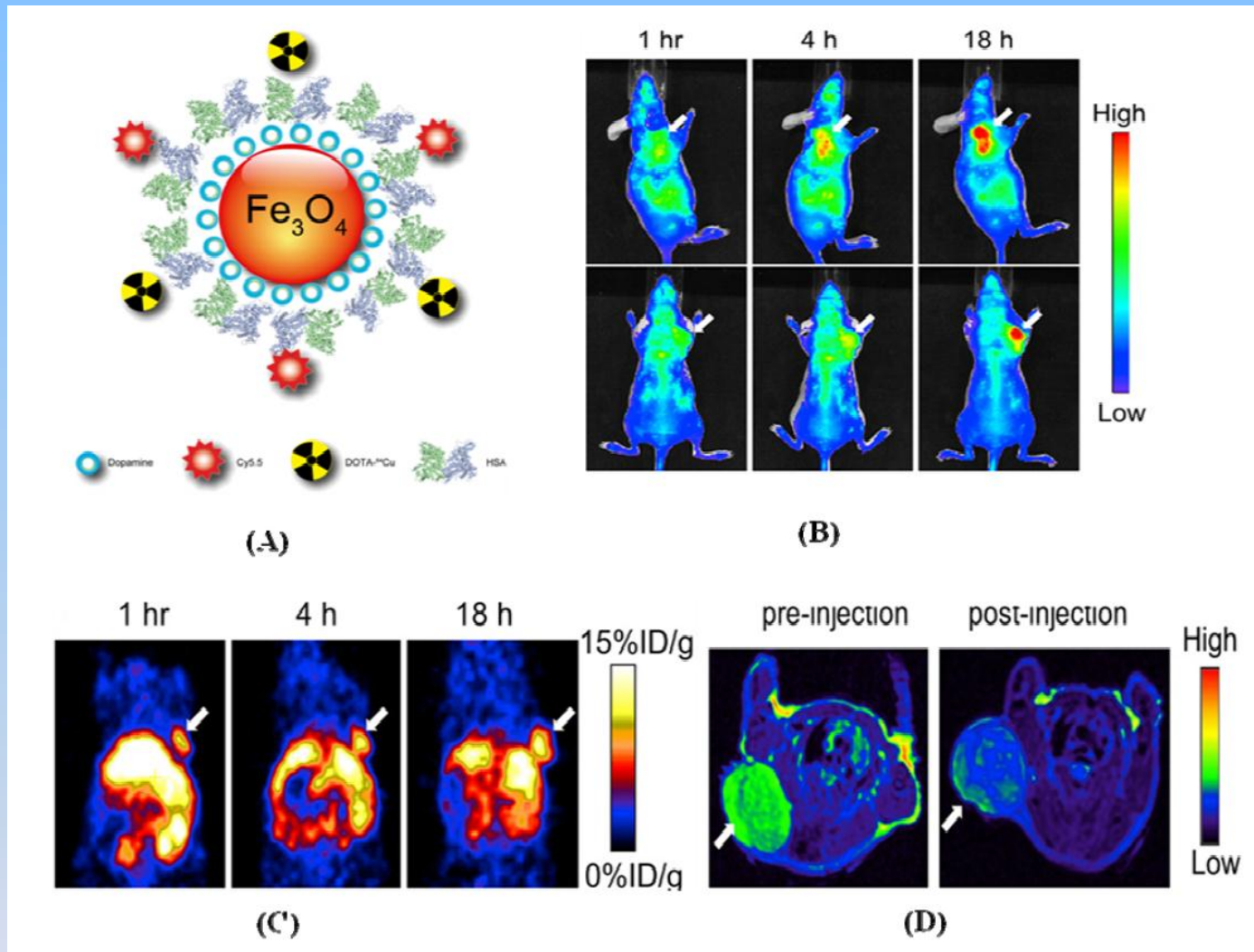
(E)



(F)

Various types of nanomaterials used as contrast agents for targeted imaging: (A) gold nanoparticle; (B) carbon nanotube; (C) liposome; (D) micelle; (E) quantum dot; and (F) dendrimer.



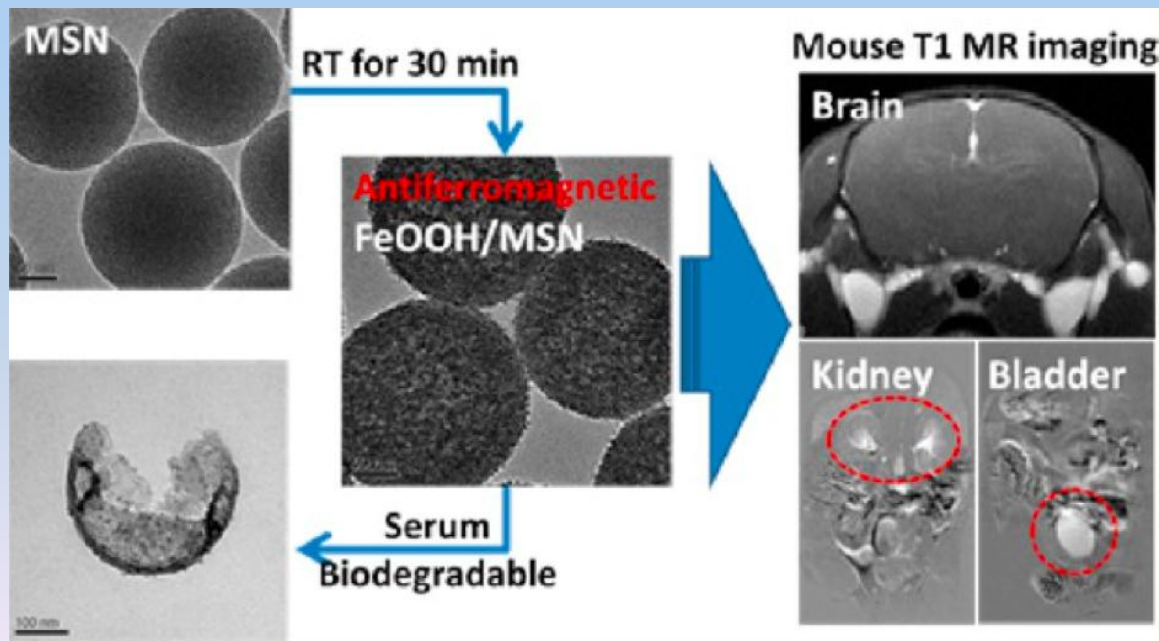


(A) Schematic representation of triple functional probe HSA-IONPs for PET/optical and MR imaging; (B) Representative *in vivo* NIR images of a mouse injected with the probe. Images were acquired 1, 4 and 18 h post-injection; (C) *In vivo* PET images of the mouse are shown after injection at 1, 4 and 18 h; (D) MR images acquired before and 18 h post-injection are shown.

# *Mesoporous silica Nanoparticles*

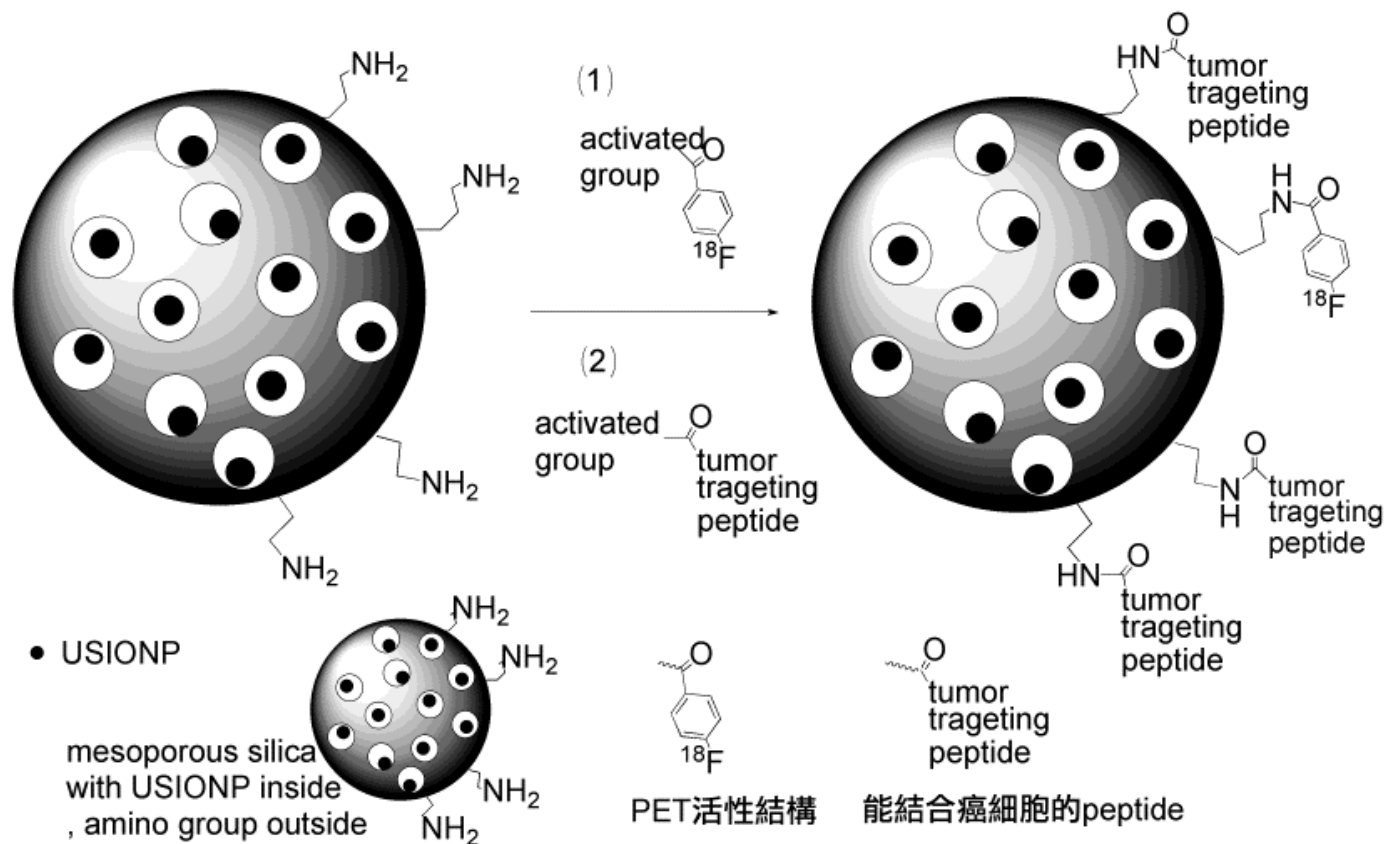
## T<sub>1</sub>-weighted MRI Contrast Agent

- 可生物分解，可腎排除
- 2nm的ultra small iron oxide nanoparticles
- 放入直徑200nm 的mesoporous silica奈米載體



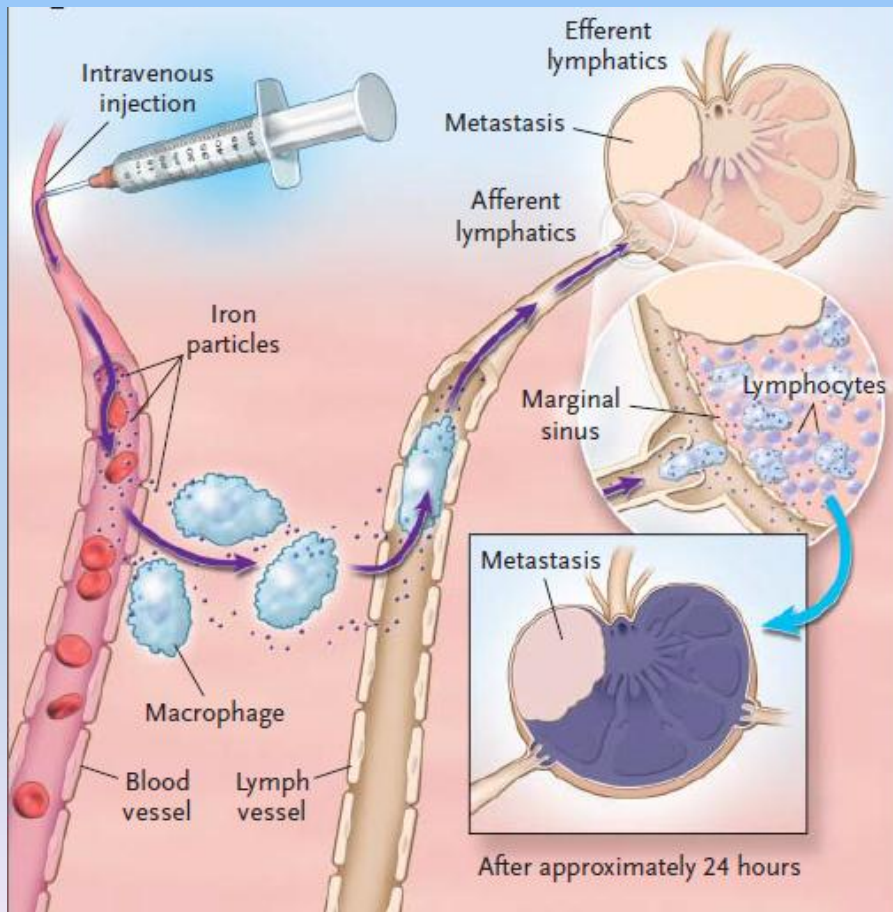
Chou PT, et al. Antiferromagnetic Iron Nanocolloids: A New Generation in Vivo T1 MRI Contrast Agent. *J. Am. Chem. Soc.* 2013;135:18621.

# 奈米載體PET/MRI顯影劑

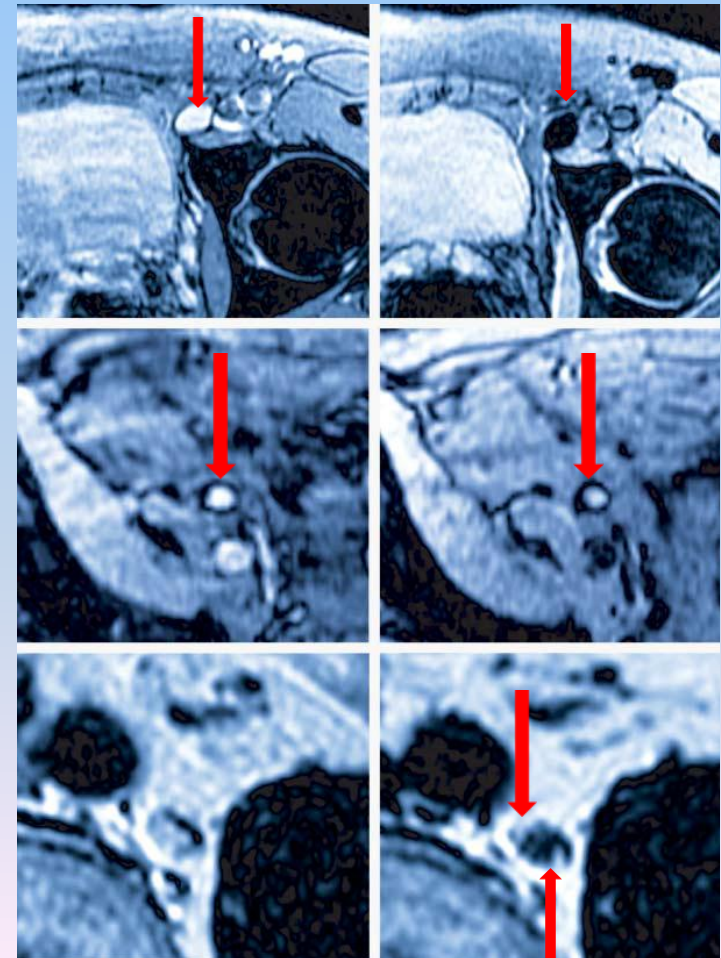




# Metastatic lymph node detection using MRI and SPIO nanoparticles

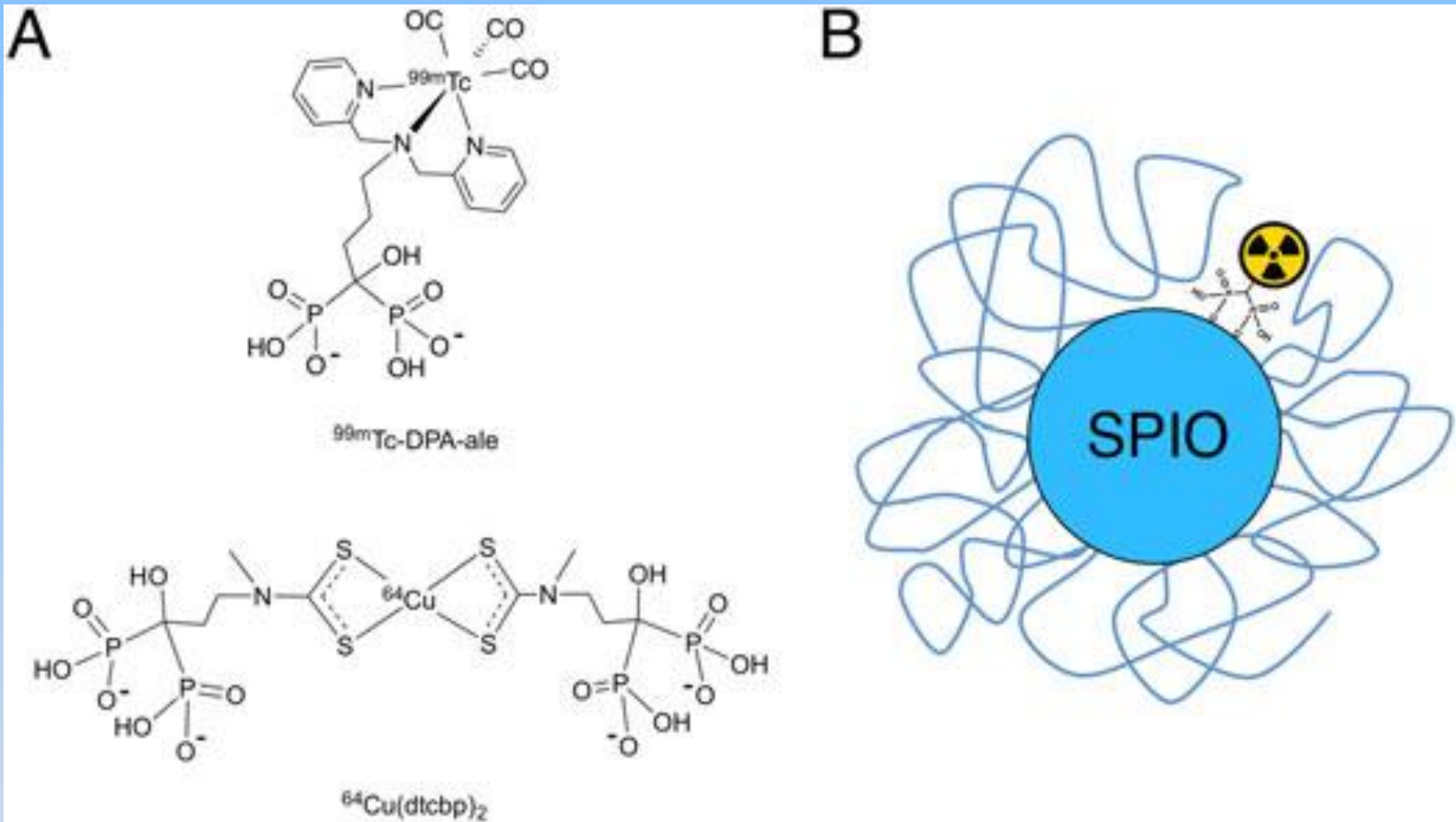


Convention MRI Post-contrast 24 hr

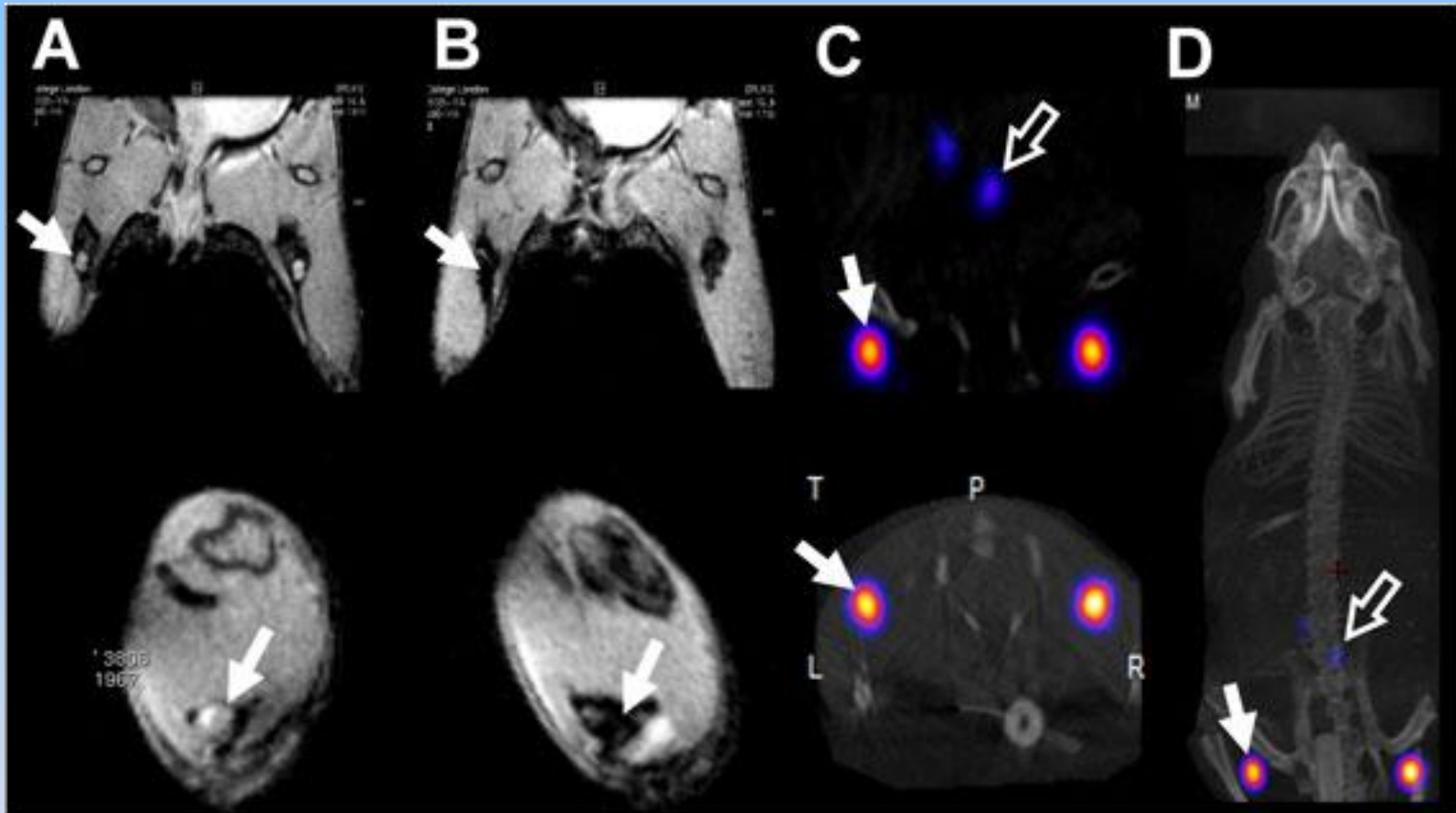


N Engl J Med 2003;348:2491-9.

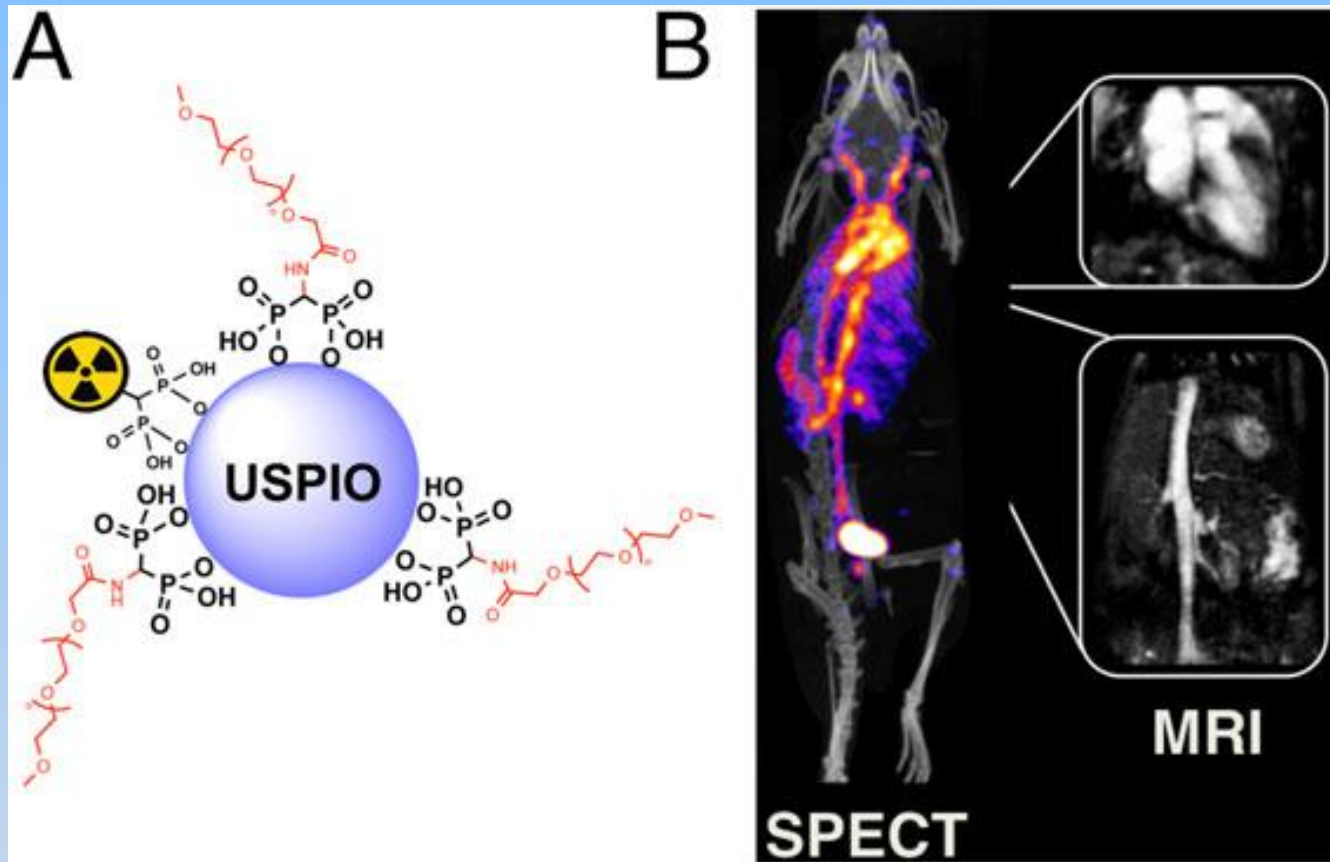




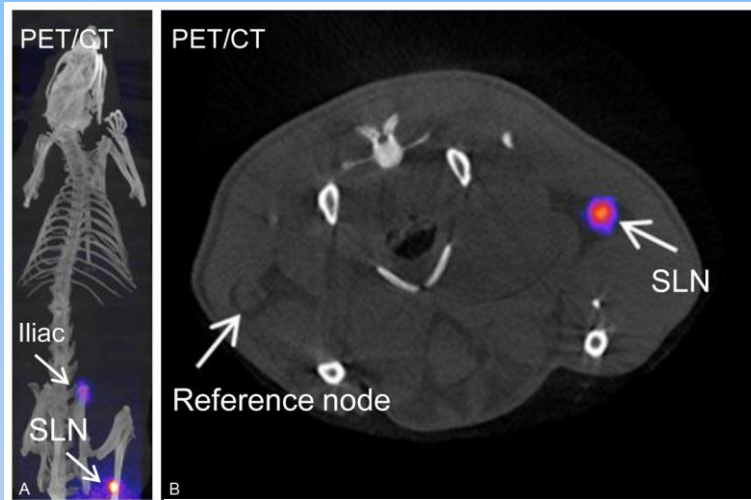
Bimodal superparamagnetic iron oxides (SPIOs) for sentinel lymph node imaging. (A) Bifunctional bisphosphonates for single photon emission computed tomography and positron emission tomography imaging used for the radiolabelling of SPIOs; (B) Schematic representation of the radiolabelled dextran-coated SPIO (Endorem/Feridex). USPIO, ultra-small SPIO.



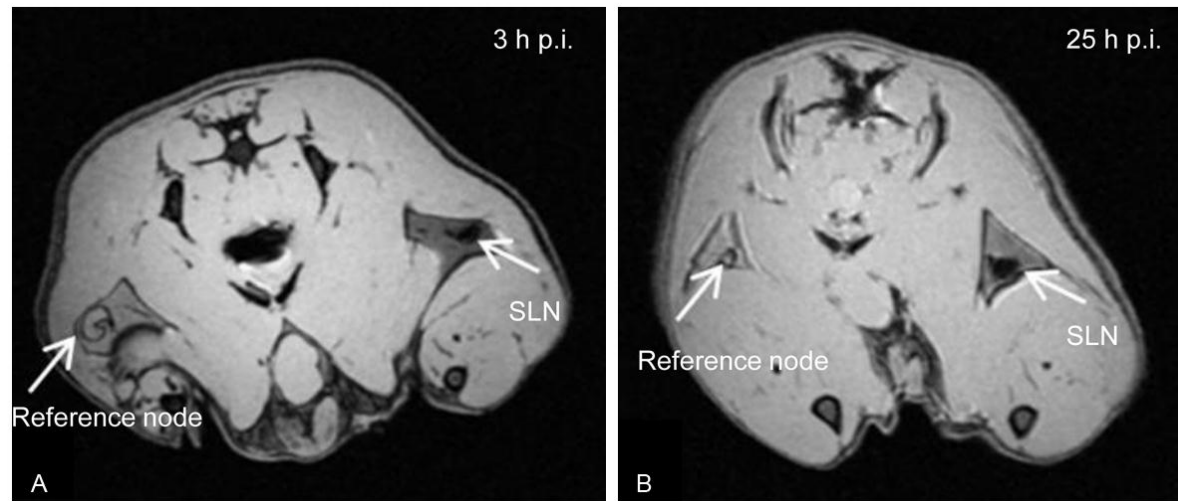
In vivo PET-MRI studies with  $^{64}\text{Cu}(\text{dtcbp})_2\text{-Endorem}$  in a mouse. (A) and (B): coronal (top) and short-axis (bottom) magnetic resonance images of the lower abdominal area and upper hind legs showing the popliteal lymph nodes (solid arrows) before (A) and after (B) footpad injection of  $^{64}\text{Cu}(\text{dtcbp})_2\text{-Endorem}$ . (C) Coronal (top) and short-axis (bottom) NanoPET-CT images of the same mouse as in B showing the uptake of  $^{64}\text{Cu}(\text{dtcbp})_2\text{-Endorem}$  in the popliteal (solid arrow) and iliac lymph nodes (hollow arrow). (D) Whole-body NanoPET-CT showing sole uptake of  $^{64}\text{Cu}(\text{dtcbp})_2\text{-Endorem}$  in the popliteal and iliac lymph nodes. No translocation of radioactivity to other tissues was detected.



Long circulating bimodal nanoparticles for PET-MR and SPECT-MRI. (A) Bisphosphonate anchors allow strong and stable binding of PEG polymers and radionuclides on the surface of the USPIOs; (B) The bimodal nanoparticles circulate in the bloodstream, as indicated by the strong imaging signal in the heart and vessels. The compound can be detected using radionuclide imaging and T1-MRI. Negligible uptake in the reticuloendothelial system was detected. USPIOs, ultra-small superparamagnetic iron oxide.



Madru R. et al.  $^{68}\text{Ga}$ -labeled superparamagnetic iron oxide nanoparticles (SPIONs) for multi-modality PET/MR/Cherenkov luminescence imaging of sentinel lymph nodes. *Am J Nucl Med Mol Imaging* 2014;4(1):60-69.

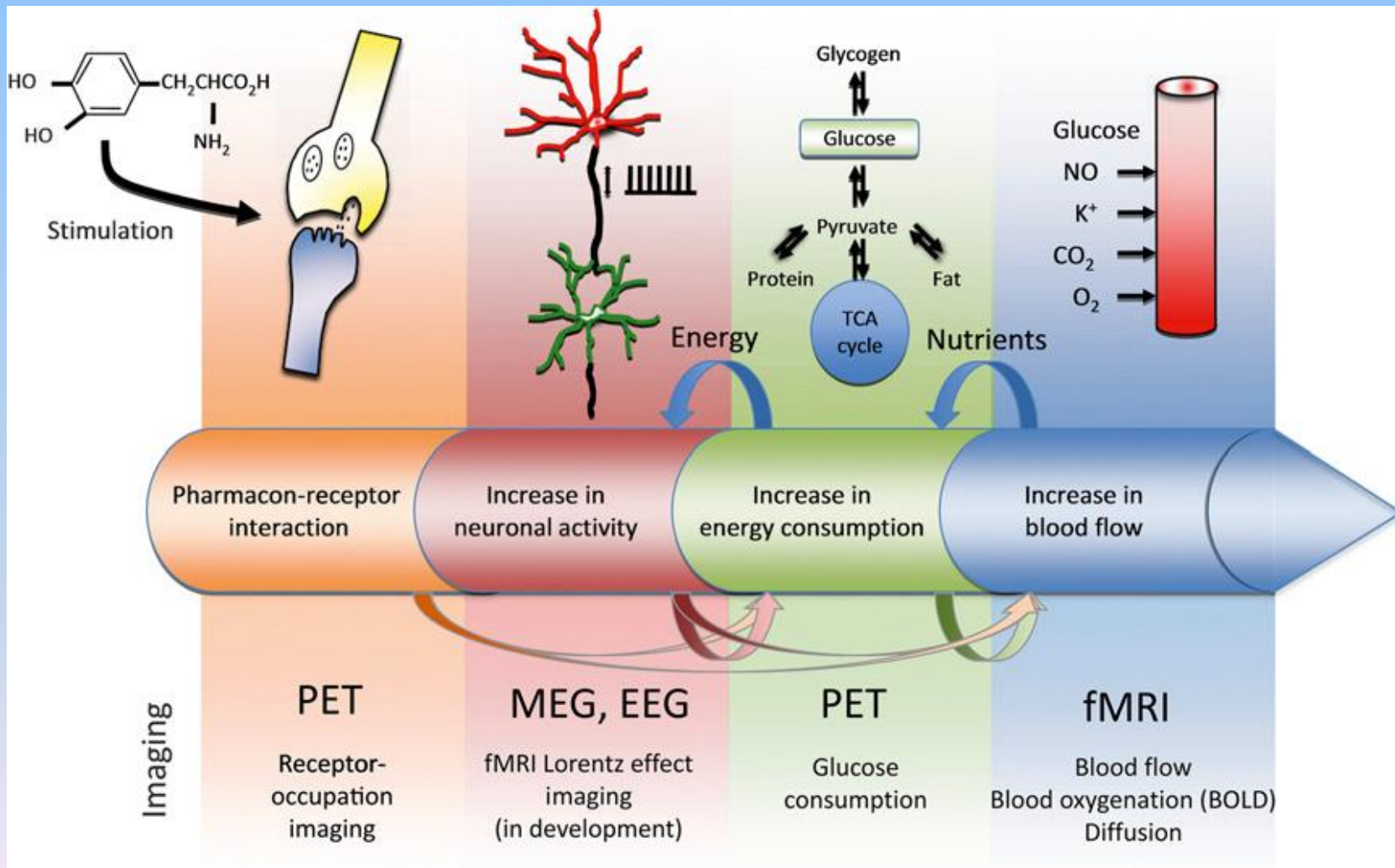


PET/CT image of one representative animal. A: Fused whole-body image of the rat 3 h after subcutaneous injection with  $^{68}\text{Ga}$ -SPIONs. The arrows show accumulation of  $^{68}\text{Ga}$ -SPIONs in the SLN (popliteal) and iliac node. B: The axial image visualizing the SLN in comparison with the contralateral reference node.

# Conclusion

- The advent of PET/MR opens new possibilities in how we used contrast agents
  - Unimodal approach: multiparametric information
  - Bimodal approach: Limited, but potentially useful applications
- Radiolabelled MRI complexes (Gd, Mn) allow the in vivo applications of responsive contrast agent (e.g. PH)
- Radiolabelled SPIOs in combination with MRI methods could be used to locate and assess the status of SLNs in several cancers
  - More effective staging and management
  - Prevent unnecessary LN excision
  - Allow the preoperative and intraoperative guidance for SLNB





*J Nucl Med.* 2014;55:40S-46S.

Thank you for your attention!!